Fluid Dynamics &
Materials Processing

Tech Science Press

http://doi.org/10.32604/fdmp.2026.082152

REVIEW

Hydrodynamic Mechanisms, Fluid–Structure Interaction, and Material Selection in Underwater Bio-Inspired Robots: A Review

Hao Jiang[1], Lucheng Sun[2], Liguo Shuai[1,*] and Zhihan Li[3,*]

[1]School of Mechanical Engineering, Southeast University, Nanjing, China
[2]School of Information Engineering, Yangzhou University, Yangzhou, China
[3]Department of Industrial and Systems Engineering, The Hong Kong Polytechnic University, Hung Hom, Kowloon, Hong Kong
*Corresponding Authors: Liguo Shuai. Email: liguo.shuai@163.com; Zhihan Li. Email: lizhihan1994@163.com

Received: 11 March 2026; Accepted: 11 June 2026; Published: 30 June 2026

ABSTRACT: Underwater bio-inspired robots have emerged as a promising alternative to conventional propeller-driven autonomous underwater vehicles and remotely operated vehicles because of their potential for high propulsive efficiency, superior maneuverability, reduced acoustic signatures, and enhanced environmental adaptability. Unlike rigid propellers operating under approximately steady inflow conditions, bio-inspired propulsion relies on strongly unsteady hydrodynamic mechanisms, including vortex generation and shedding, added-mass effects, boundary-layer evolution, and flexible fluid–structure interaction (FSI). These processes fundamentally govern thrust production, energy conversion, and maneuvering performance, yet a systematic synthesis connecting hydrodynamic mechanisms with engineering implementation remains limited. This review addresses that gap from a hydrodynamic perspective. First, the major propulsion modes of aquatic organisms, including body and caudal fin (BCF), median and paired fin (MPF), and jet propulsion, are summarized together with their characteristic wake structures. Key unsteady flow mechanisms are then discussed, including reverse Kármán vortex streets, leading-edge vortex dynamics, dynamic stall, boundary-layer behavior, wake instabilities, and biomimetic drag-reduction strategies. Particular attention is given to flexible FSI, including modeling frameworks, passive deformation–active actuation coupling, stiffness and morphology effects, and energy-transfer pathways. Representative studies report propulsive efficiencies of approximately 50–70% for optimized flexible flapping foils and above 70% for phase-tuned dual-foil systems, while biomimetic surface designs have achieved approximately 5–10% drag reduction under specific flow conditions. However, these gains remain strongly condition-dependent, and their practical transfer is still limited by scale effects, propulsor interference, model uncertainty, material degradation, biofouling and insufficient marine validation. Future directions are proposed in real-environment hydrodynamics, multi-robot flow coordination, interdisciplinary modeling, and advanced materials. This review provides a mechanism-to-design framework for understanding, designing, and optimizing next-generation underwater bio-inspired robots.

KEYWORDS: Bio-inspired underwater robots; unsteady hydrodynamics; fluid–structure interaction; flexible propulsion; biomimetic materials

1 Introduction

Underwater robots are instrumental in marine exploitation, resource exploration, and subsea operations, driving an escalating demand for extended endurance, high propulsion efficiency, reduced acoustic signatures, and superior maneuverability [1–3]. Conventional Autonomous Underwater Vehicles (AUVs) and Remotely Operated Vehicles (ROVs) predominantly utilize rigid hulls and propeller-based propulsion [2,3]. However, rotary propellers often exhibit compromised efficiency and stability during low-speed

Copyright © 2026 The Authors. Published by Tech Science Press. This work is licensed under a Creative Commons Attribution 4.0 International License, which permits unrestricted use, distribution, and reproduction in any medium, provided the original work is properly cited.

maneuvering. Furthermore, in complex environments, they pose a risk of damaging aquatic ecosystems or becoming entangled in aquatic vegetation [2–4]. In contrast, aquatic organisms such as fish have evolved over millions of years to achieve efficient propulsion through the oscillation of caudal and pectoral fins. These biological systems demonstrate exceptional maneuverability and environmental adaptability [5–7]. Extensive experimental measurements indicate that the propulsive mechanical efficiency of certain high-speed swimmers, such as thunniform fish, can reach 80–90%, significantly surpassing that of conventional screw propellers (approximately 50–70%) [8–10]. Additionally, species like swordfish are capable of achieving instantaneous bursts of speed up to 110 km/h [11,12]. These results indicate that bio-inspired propulsion strategies might have different benefits regarding energy utilization. However, replicating these remarkable biological capabilities in engineered systems remains challenging. A key scientific bottleneck lies in the insufficient understanding of the fundamental differences between steady-state and unsteady-state hydrodynamic mechanisms, particularly the latter's decisive role in propulsion performance. Traditional propellers operate under near-steady inflow conditions and are typically designed using stable airfoil theory [10]. In contrast, biomimetic propulsion involves intense unsteady flow and vortex dynamics, with thrust generation dependent on acceleration and the instantaneous reaction force generated by periodic vortex shedding [13,14]. The complexity of these unsteady fluid-structure interaction (FSI) mechanisms makes analytical solutions difficult, resulting in limited understanding of the underlying principles of efficient bio-propulsion [14–17]. Therefore, a comprehensive review of unsteady flow mechanisms in underwater biomimetic robots from a fluid dynamics perspective is essential. Such analyses aim to elucidate the inherent vortex dynamics and fluid-structure interaction laws in flexible biomimetic propulsion [15,16].

Bio-inspired underwater robotics has advanced rapidly in propulsion hydrodynamics, flexible appendage design, fluid-structure interaction, drag reduction, and functional materials [17,18]. However, these topics are often treated separately, and their mechanistic links remain insufficiently synthesized [1,8]. Based on this deficiency, this paper re-examines the research on biomimetic underwater robots from a hydrodynamic perspective, focusing on propulsion methods, vortex-induced thrust generation, flexible fluid-structure interaction, and material surface manipulation [13]. The peer-reviewed studies reviewed here are classified according to propulsion mode, dominant unsteady flow mechanism, FSI strategy, energy-utilization pathway, and surface-material design [19,20]. The novelty of this review lies in integrating these aspects to clarify how microscopic flow mechanisms and flexible structural responses determine macroscopic propulsion performance and engineering limitations. The paper is organized as follows: Section 2 outlines the primary bio-inspired propulsion modes and the characteristic unsteady flow fields they generate; Section 3 delves into unsteady hydrodynamic mechanisms, including vortex dynamics, boundary layer behavior, and flow instability; Section 4 focuses on the fluid-structure interactions and energy efficiency of flexible propulsion structures; Section 5 examines the role of deformable soft materials and bio-inspired surfaces in underwater propulsion; Section 6 summarizes the limitations of current research and proposes future research directions; finally, Section 7 provides concluding remarks and implications for researchers.

2 Bio-Inspired Propulsion Modes and Unsteady Flow Fields

Aquatic organisms have evolved diverse locomotion modes, which can be categorized into distinct kinematic forms of propulsion mechanisms [21–24]. The seminal work by Breder and Webb classifies fish swimming modes into two primary categories based on the dominant propulsive structures: Body and Caudal Fin (BCF) propulsion and Median and Paired Fin (MPF) propulsion [25]. In the BCF mode, propulsion is primarily generated by the undulation of the body trunk and the oscillation of the caudal fin.

Conversely, the MPF mode relies on the undulation or oscillation of median fins (dorsal, anal) or paired fins (pectoral, pelvic) to generate thrust [23–26].

Based on the amplitude of their body swaying, BCF propulsion can be further subdivided into anguilliform, subcarangiform, carangiform, thunniform, and ostraciiform modes [23,24]. Anguilliform swimmers (e.g., eels) exhibit large-amplitude undulations along the entire body length, achieving relatively high speeds [23,24]. In contrast, subcarangiform and carangiform swimmers restrict undulation to the posterior one-half or one-third of the body, typically operating at higher tail-beat frequencies [23,24]. Thunniform swimmers (e.g., tuna) derive propulsion almost exclusively from the high-speed oscillation of a stiff, powerful caudal fin, with estimated mechanical efficiencies as high as 80–90% [8–10,24]. Ostraciiform swimmers (e.g., boxfish, cowfish) possess rigid bodies and rely on small-amplitude caudal fin oscillations for low-speed locomotion [23,24]. In contrast, MPF modes encompass rajiform, diodontiform, amiiform, gymnotiform, balistiform, and labriform swimming styles. The former categories generate propulsion via the undulation of dorsal, anal, or pectoral fins (e.g., the spanwise undulation of the manta ray's broadened pectoral fins) [25–27]. The latter types, such as wrasses and parrotfish, generate thrust through rapid pectoral fin flapping mechanisms [24,28]. Generally, BCF modes excel in high-speed cruising and propulsive efficiency, whereas MPF modes are superior for low-speed maneuvering and station-keeping stability [28–30]. Each biomimetic propulsion category possesses distinct characteristics: for instance, BCF swimmers like tuna generate powerful periodic wake jets via tail oscillation, yielding significantly higher efficiency during sustained cruising compared to propeller-driven submersibles [8,9,29]. Conversely, MPF swimmers such as boxfish and manta rays utilize the coordinated control of multiple fins to achieve agile turning and hovering—capabilities that are difficult for propeller-driven underwater robots to replicate [30,31]. To systematically demonstrate this diversity, Fig. 1 presents a comprehensive overview of the primary bio-inspired propulsion modes alongside their corresponding representative robotic prototypes.

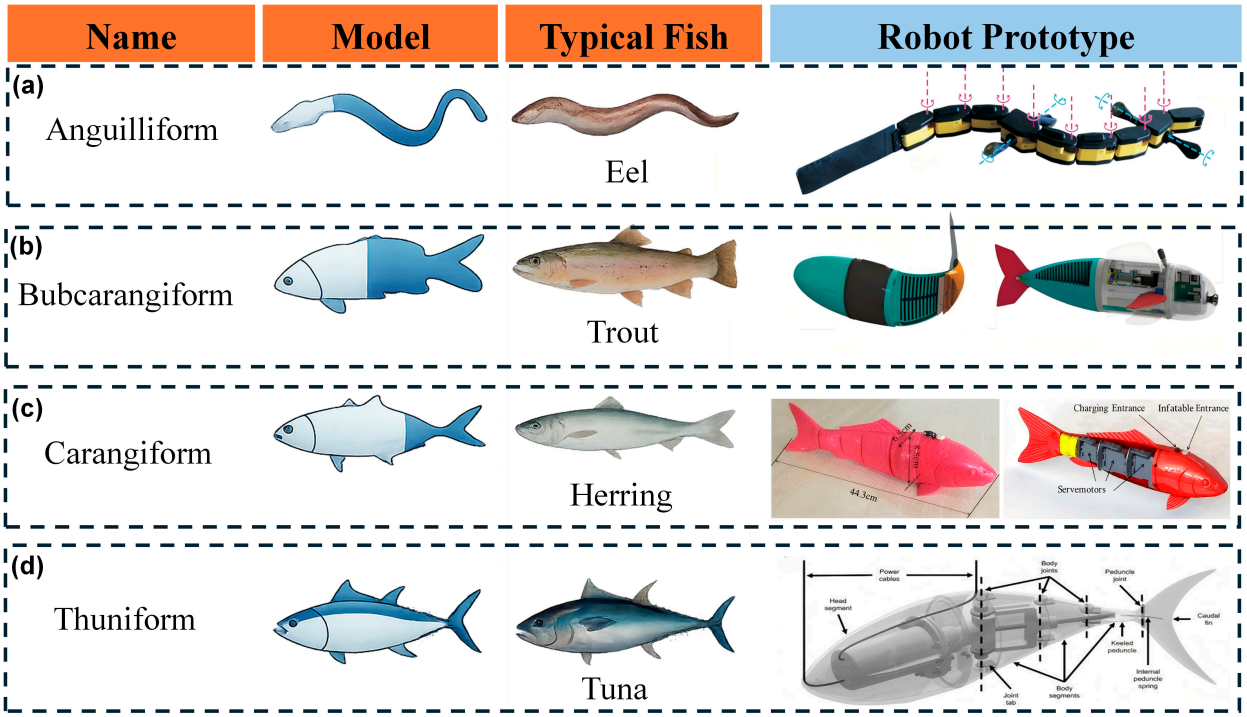

Figure 1: *Cont.*

Figure 1: Classification of fish-inspired propulsion modes and representative robots. (**a**) ACM-R5 snake-like robot. (**b**) MIT soft robotic fish. (**c**) Robotic Koi. (**d**) Tunabot Flex. (**e**) Robotic Boxfish. Panels (**a**–**e**) are adapted with permission from Refs. [32–36], respectively.

In addition, some organisms in nature utilize jet propulsion, such as cephalopods like squid and octopus, and gelatinous organisms like jellyfish [37,38]. This propulsion mode typically involves a two-phase cycle comprising "intake/refilling" and "contraction/jetting" [39–41]. During the jetting phase, shear layers at the nozzle roll up to form vortex rings. Subsequently, these vortex rings detach and organize into strings of vortex rings in the wake, thereby facilitating momentum transfer and propulsion [39–42]. This unique hydrodynamic mechanism, characterized by the shearing of pulsed vortex rings, has inspired the development of various soft and smart material-driven marine robots, as shown in Fig. 2.

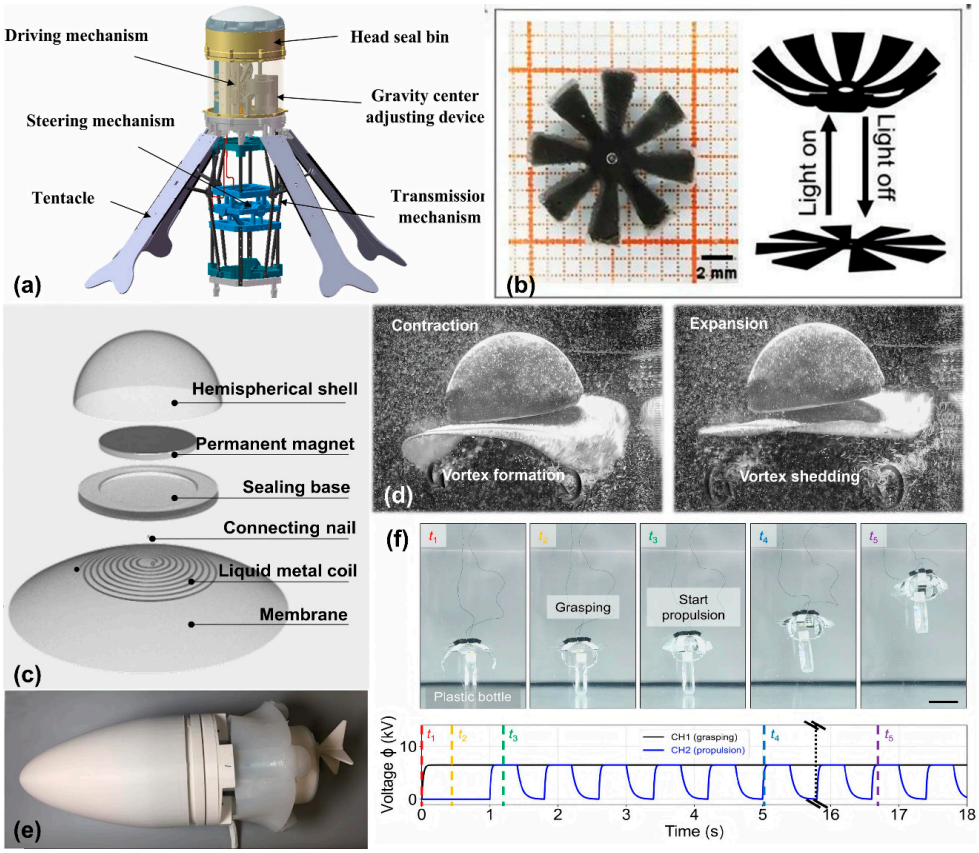

Figure 2: Bio-inspired jet propulsion and invertebrate soft robots. (**a**) Linkage-driven biomimetic jellyfish robot. (**b**) Fully soft LM-Jelly with liquid-metal electromagnetic actuation. (**c**) Light-driven hydrogel jellyfish robot. (**d**) Dye visualization of vortex-ring formation and shedding. (**e**) Cephalopod-inspired soft jet robot with a deformable mantle. (**f**) HASEL-driven jellyfish robot for underwater manipulation. Scale bar, 5 cm. Panels (**a**–**f**) are adapted with permission from Refs. [43–47], respectively.

To provide a clearer comparison of these propulsion modes, Table 1 summarizes their main mechanisms, advantages, limitations, and potential robotic applications. BCF propulsion is generally suitable for efficient cruising and strong thrust generation, MPF propulsion is more advantageous for maneuvering and station keeping, whereas jet propulsion provides a compact and compliant solution for soft-bodied underwater robots.

Table 1: Simplified comparison of major bio-inspired propulsion modes for underwater robots.

Propulsion Mode	Main Mechanism	Advantages	Limitations	Typical Applications
BCF	Traveling wave oscillation	High speed; High efficiency; Strong thrust	Poor hovering; Wide turning; Hard control	Long-range cruise
MPF	Symmetrical flapping	High maneuverability; hovering stability; Station keeping;	Lower speed; Weak thrust; Fin coupling	Precise inspection
Jet	Intake-contraction pulse	Compact structure; Burst motion; Soft compliance	Refill loss; Low endurance; Pulsed thrust	Short-range burst

3 Unsteady Hydrodynamic Mechanisms

Flows associated with bio-inspired propulsion are strongly unsteady, featuring vortex generation and evolution, boundary-layer separation and reattachment, and wake instabilities. These phenomena are intimately linked to thrust production and maneuvering performance. The following sections discuss these aspects in detail.

3.1 Vortex Dynamics and Thrust Generation in Flapping Fins

The propulsion of fish caudal fins or bio-inspired robotic foils is fundamentally predicated on the momentum exchange resulting from the generation and shedding of periodic vortex structures [13,48–50]. When a flexible fin or foil oscillates laterally at a specific frequency, an alternating vortex street forms in the wake [13,48]. A pattern that transports fluid momentum downstream—generating net thrust—is termed a Reverse Kármán vortex street, whereas a conventional Kármán vortex street corresponds to drag generation [13,48]. Particle Image Velocimetry (PIV) measurements of the wakes of high-speed cruisers, such as tuna, clearly reveal regular reverse Kármán vortex trains and concentrated backward-directed jets [48,49]. Such ordered vortex streets are hallmarks of high propulsive efficiency, the formation of which requires kinematic parameters, such as flapping frequency and amplitude, to fall within an optimal range [50–52]. The flapping kinematics are typically characterized by the dimensionless Strouhal number, defined as $St = fA/U$, where f is the oscillation frequency, A is the peak-to-peak tail amplitude, and U is the forward swimming speed [50,51]. Extensive experimental and numerical studies demonstrate that bio-inspired propulsive efficiency peaks within the range of $St \approx 0.2-0.4$. For instance, Schouveiler et al. (2005) reported mean propulsive efficiencies exceeding 70% for an oscillating hydrofoil under optimal parameters [51]. Furthermore, dual-propulsor experiments by Mannam et al. (2017) indicated a maximum efficiency of approximately 73% at $St \approx 0.225$, with efficiency declining as frequency increased further. It can be observed that at $St < 0.2$, efficiency is low due to insufficient wake momentum and thrust. As St increases, efficiency rises, reaching a peak of 70–80% around $St \approx 0.25$. Beyond this point, excessive frequency leads to chaotic vortex structures and increased energy dissipation, causing a decline in efficiency [49–52]. These results

are corroborated by numerous bio-inspired propulsion experiments [49,51,52]. Consequently, modulating kinematic parameters to maintain a stable, ordered reverse Kármán vortex street in the wake is a critical mechanism for achieving high-efficiency thrust generation [13,48–50]. The intricate relationship between these kinematic parameters, the resulting three-dimensional wake topologies (such as the reverse Kármán vortex street), and the corresponding propulsive efficiency envelopes is visually elucidated in Fig. 3.

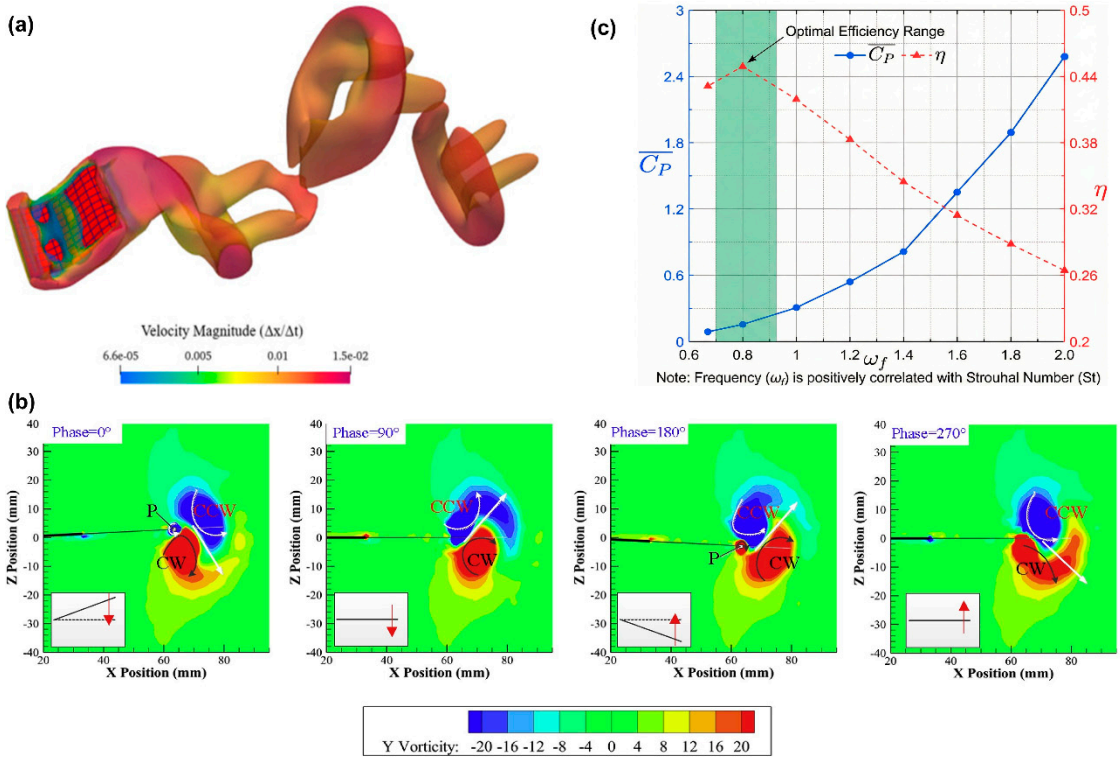

Figure 3: Unsteady vortex wakes and efficiency characteristics in biomimetic propulsion. (**a**) Three-dimensional vortical structures of a flexible flapping propulsor visualized by Q-criterion iso-surfaces. (**b**) Mid-plane vorticity contours of a biomimetic caudal fin showing alternating vortex shedding. (**c**) Propulsion efficiency as a function of oscillation frequency, indicating an optimal Strouhal-number range. Panels (**a**–**c**) are adapted with permission from Refs. [13,17,27], respectively.

Another significant source of unsteady thrust is the acceleration reaction force [53]. Specifically, as the fin accelerates, it exerts added mass forces on the surrounding fluid, generating instantaneous thrust [53]. At the onset of each oscillation half-cycle, pressure on the windward side of the fin increases sharply—creating an impulsive pressure wave akin to "pushing" the water mass. Subsequently, the shear layer at the fin edge rolls up to form a Leading-Edge Vortex (LEV). This vortex remains attached to the suction side of the fin, creating a low-pressure region that contributes an additional component of lift and thrust during the acceleration phase [48,50,54]. This process is analogous to the dynamic lift overshoot observed during the rapid startup of airfoils. As the stroke reverses, the previously formed LEV is eventually shed from the trailing edge and coalesces with the wake vortex street. The cyclic generation and shedding of LEVs cause the fin to experience positive and negative thrust phases within each period [48,49,54]. During the initial acceleration, net thrust is positive as the fin accelerates the fluid backward. However, at the moment of stroke reversal and deceleration, fluid inertia can induce instantaneous drag (negative

thrust) on the fin [49,54]. Nevertheless, provided that the flapping parameters are optimal, the positive thrust phase dominates while the negative phase is suppressed, resulting in a net positive cycle-averaged thrust [49–52]. Flexible fins exhibit significant advantages in this regard: due to structural elasticity, there is a phase lag between the kinematic properties of the fin and the hydrodynamic forces. This lag can more effectively direct the force vector in the swimming direction, thereby reducing the reverse drag during the stroke reversal [14,55]. Comparative experiments show that, at the same frequency, the average net thrust generated by flexible fins is several times higher than that of rigid fins of the same size [14,56]. This is partly attributed to the ability of flexible structures to "filter" thrust fluctuations: strain energy is stored during the propulsion phase and released during the stroke reversal phase, resulting in a smoother and more continuous thrust output [14,55,56]. In summary, the unsteady thrust sources of biomimetic fins can be divided into two parts: the average thrust generated by the backward momentum flux of the vortex street wake, and the transient thrust caused by the added mass effect and leading-edge vortex attachment during fin acceleration. By optimizing the fin stiffness distribution and kinematic parameters to synchronize the phases of these two mechanisms, propulsion efficiency and thrust magnitude can be significantly improved [53,55,56].

From the perspective of dimensionless kinematic parameters, the propulsive efficiency of oscillating fins or wings typically exhibits a unimodal dependence on the Strouhal number. Within an intermediate St range, the phase and shedding scale of wake vortices align optimally with fin kinematics, thereby facilitating superior thrust-to-power conversion efficiency. Conversely, at excessively low or high St values, efficiency declines significantly due to distinct hydrodynamic mechanisms: low St regimes are characterized by insufficient vortex strength and limited momentum exchange, whereas high St regimes suffer from desynchronized vortex shedding and intensified deleterious vortex interference [49–52].

3.2 Boundary Layer Behavior and Dynamic Stall

Boundary layer separation and stall phenomena on bio-inspired propulsion surfaces exert a profound influence on propulsive forces [15,57]. Under steady conditions, if the angle of attack (AoA) of an airfoil exceeds a critical value, stall occurs, characterized by a precipitous drop in lift and a surge in drag [57,58]. However, during unsteady flapping, the interplay of kinematics and vortex dynamics imparts distinct characteristics to dynamic stall [57,59]. Even when the instantaneous AoA exceeds the static stall threshold, the generation of a LEV often delays flow separation, thereby sustaining high lift for a prolonged duration [14,57,59]. Studies demonstrate that oscillating hydrofoils can temporarily withstand angles of attack significantly surpassing the static stall angle without undergoing complete stall. Consequently, the mean lift coefficients can exceed those of a static foil at equivalent angles by several fold. For instance, experimental investigations by Young et al. (2019) on an oscillating NACA0012 foil revealed that, with the AoA varying cyclically between 0° and 20°, the mean lift was approximately six times higher than that of the static case [60]. This enhancement effect is attributed to the leading-edge vortex (LEV) formed during the acceleration phase, which remains attached to the wing surface [14,54,57,59]. This vortex effectively alters the direction of the incoming flow, thereby temporarily increasing the slope of the lift curve [59,61]. Stall only occurs when the vortex detaches, and the wing begins to decelerate and reverse. Organisms have evolved the ability to utilize this unstable delayed stall mechanism [54,59]. For example, the principle by which fruit flies generate leading-edge vortices to maintain high lift is similar to the hydrodynamic characteristics of fish fins during rapid acceleration maneuvers [54,59,62]. For underwater biomimetic robots, the clever use of dynamic stall can generate enormous instantaneous thrust when needed (e.g., during rapid starts or sharp turns) [59,62]. However, this also comes with risks such as structural vibrations

and instabilities caused by vortex detachment [14,59,63]. Fig. 4 graphically illustrates the formation of LEV and its key role in delayed dynamic stall, revealing how transient pressure distribution anomalies lead to a significant increase in transient hydrodynamic loads.

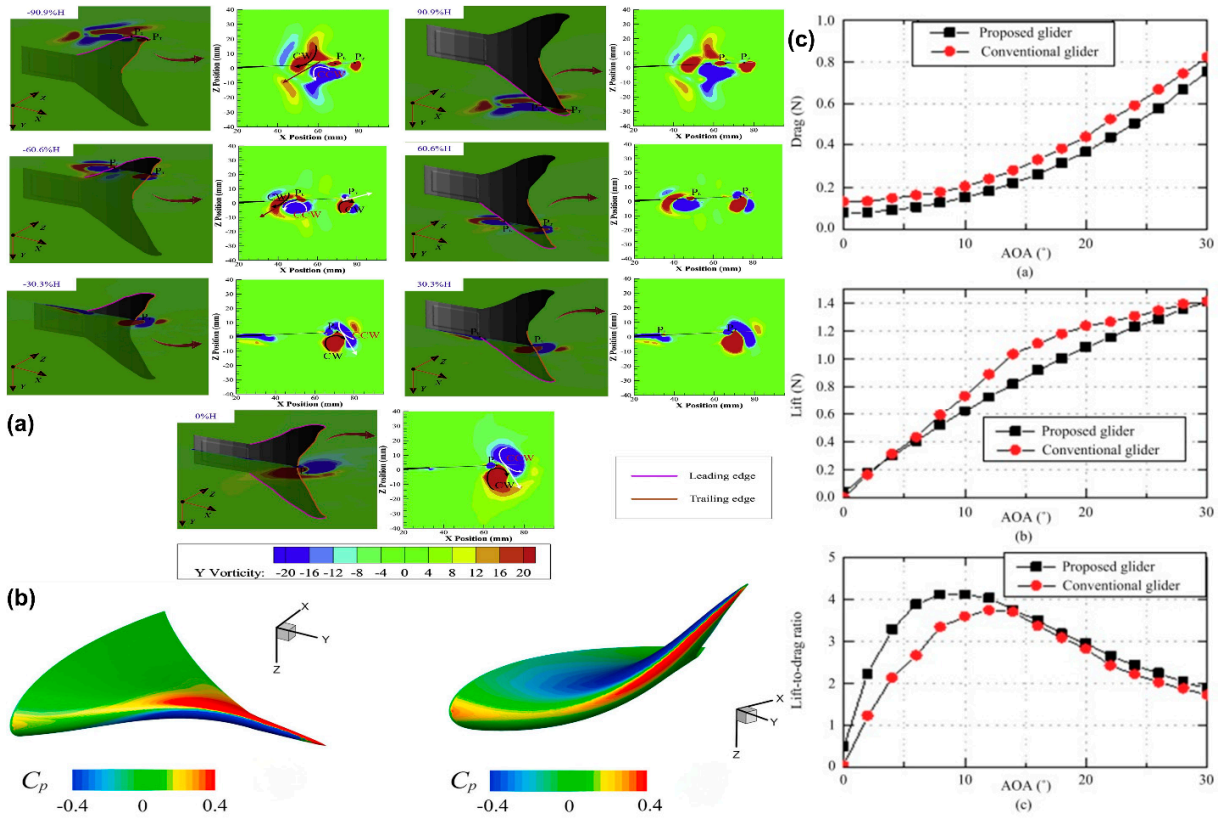

Figure 4: LEV dynamics and angle-of-attack-dependent hydrodynamic forces. (**a**) Instantaneous vorticity fields showing LEV formation and attachment around the biomimetic propulsor. (**b**) Surface pressure distribution at different phases, with low-pressure regions associated with the LEV core. (**c**) Variation of lift and drag forces with angle of attack. Panels (**a**–**c**) are adapted with permission from Refs. [13,27,64], respectively.

Furthermore, the boundary layer state has a crucial impact on propulsion efficiency [65,66]. Smooth, rigid surfaces typically undergo laminar-turbulent transitions and separation at specific Reynolds numbers [67]. In contrast, biological surfaces often possess unique compliance and microstructures that can modulate boundary layer evolution, thereby delaying separation and reducing energy dissipation [18,19,65,66]. A prime example is the micron-scale ribbed structure on shark skin, which can reduce turbulent surface friction drag by approximately 5% to 8% [68,69]. The underlying mechanism involves suppressing spanwise translation of near-wall vortices [18,69]. Similarly, dolphin skin is thought to function as a compliant wall: it undergoes micro deformation in response to flow fluctuations, thereby suppressing disturbance energy and delaying the laminar-turbulent transition [18,67,70]. Biomimetic robots can enhance boundary layer properties by mimicking these strategies through advanced material and structural design [18,19,66]. For example, applying elastic coatings or flexible scale arrays to the propulsion surface can respond adaptively to changes in local pressure distribution during the flapping fin cycle, thereby extending the flow adhesion time [18,19,71]. It is worth noting that without proper design or control, boundary layer instability can have adverse effects: the formation of localized separation bubbles can lead to irregular vortex shedding, resulting

in thrust fluctuations and reduced efficiency [65,72]. Therefore, understanding and controlling boundary layer behavior during unsteady flapping fin processes is a key scientific challenge for improving biomimetic propulsion performance [18,65,66]. Currently, experimental studies on dynamic stall and transient boundary layer characteristics mainly focus on airborne flapping fins [72,73]. Underwater comparative experiments at high Reynolds numbers remain very limited [74,75]. Future research needs to combine PIV measurements with high-frequency pressure measurements to elucidate these details of biomimetic fins [65,76].

3.3 Flow Field Instabilities and Maneuverability

Unsteady propulsive flow fields exhibit a rich variety of instability modes. While these instabilities may compromise propulsive efficiency, they also harbor significant potential for maneuvering control [14,77]. Taking the bio-inspired caudal vortex street as an example, when the flapping frequency or amplitude deviates from optimal values, the wake vortex structures become disordered. Phenomena such as phase drift in vortex shedding and jet deflection emerge, leading to an erratic propulsion direction and reduced efficiency [77]. This is particularly pronounced for rigid caudal fins at high frequencies. Due to their inability to undergo coordinated deformation, the generated vortex rings often interfere with one another, causing the wake to exhibit a zig-zag deflection—commonly referred to as vortex street offset or wake meandering [77]. Experimental observations indicate that the jet in the wake of a rigid oscillating wing oscillates laterally, causing the thrust vector to deviate periodically and augmenting swimming resistance [77]. Conversely, flexible caudal fins can mitigate such instabilities to a certain extent by undergoing moderate deformation during vortex shedding [14,77]. The passive deformation of the flexible fin tip increases the spacing between consecutive vortices and promotes a more regular arrangement, resulting in a more rectified wake jet [77]. For instance, experiments by Shinde et al. (2014) demonstrated that a rigid wing equipped with a flexible trailing extension exhibits larger initial spacing between wake vortex rings compared to a purely rigid wing. Consequently, shed vortices are subject to a downstream "transport" effect rather than lingering, thereby preventing the meandering deflection of the jet [77]. This phenomenon elucidates that introducing structural flexibility can attenuate the detrimental effects of flow instability modes on propulsion, yielding a more stable thrust output [14,77].

On the other hand, flow field instability also provides avenues for maneuverability control. Fish often achieve rapid turns by intentionally disrupting the symmetry of vortex patterns [63,78,79]. For example, in a C-shaped initiation maneuver, a sudden lateral bend of the body induces a large-scale vortex ring on one side, generating a torque that drives the body to turn [78,79]. This pulsed maneuver relies heavily on the action of unsteady vortex forces [78,79]. Bionic robots can simulate this strategy by utilizing asymmetric oscillations to generate specific unstable flow patterns, thereby obtaining lateral forces or torques [28,80–82]. For example, a biomimetic boxfish robot uses asymmetric oscillations of its dorsal fin to induce deflecting wake vortices, thus achieving zero-radius turns [80,81]. Similarly, studies have shown that by altering the relative phase of the pectoral fins, controllable turns can be achieved by utilizing vortex asymmetry, thereby generating vortex rings of varying sizes and net lateral forces [28,82]. As shown in Figs. 5 and 6, the ingenious use of this asymmetric vortex shedding and flow instability provides a powerful fluid dynamics basis for performing highly flexible maneuvers such as rapid C-starts and sharp turns.

Furthermore, the coexistence of multiple propulsors (e.g., dorsal and caudal fins in fish, or multi-fin arrays in robots) introduces mutual interference as an additional source of flow instability [26,83]. If properly designed, this interference can be harnessed to enhance thrust or efficiency via constructive interference [26,83]. Lua et al. (2016) showed that for two oscillating wings in tandem, the interaction between the downstream wing and the upstream wake leads to constructive thrust superposition, increasing

the overall thrust coefficient [83]. Another study found that dual flexible flapping wings could achieve a propulsion efficiency of approximately 55%, compared to roughly 40% for a single wing; optimizing the phase offset between wings further increased this efficiency to 73% [84]. These results indicate that vortex interactions between multiple propulsion units can be modulated to achieve super-additive propulsion gains [83,84]. This principle holds significant implications for multi-fin robotic fish and even bio-inspired robotic swarms: rationally guiding mutual wake interference may reduce collective energy consumption and improve propulsive efficacy [26,63,83,84]. Recent fish schooling experiments reveal that the average tail-beat energy consumption of individuals in a school is reduced by 30–50% compared to solitary swimming, a reduction attributed to beneficial vortex interactions facilitated by the school's formation [85,86]. More recently, Lin et al. numerically investigated the collective motion of two freely moving parallel fish and showed that wavelength and phase difference can determine stable formations, swimming-speed modes, and energy-efficiency variations, further highlighting the importance of phase regulation in wake-mediated collective propulsion [87]. Although hydrodynamic coordination in bio-inspired robotic swarms remains a nascent field, such research highlights the immense potential of actively exploiting flow field instabilities to enhance maneuverability and collective efficiency [63,85,86].

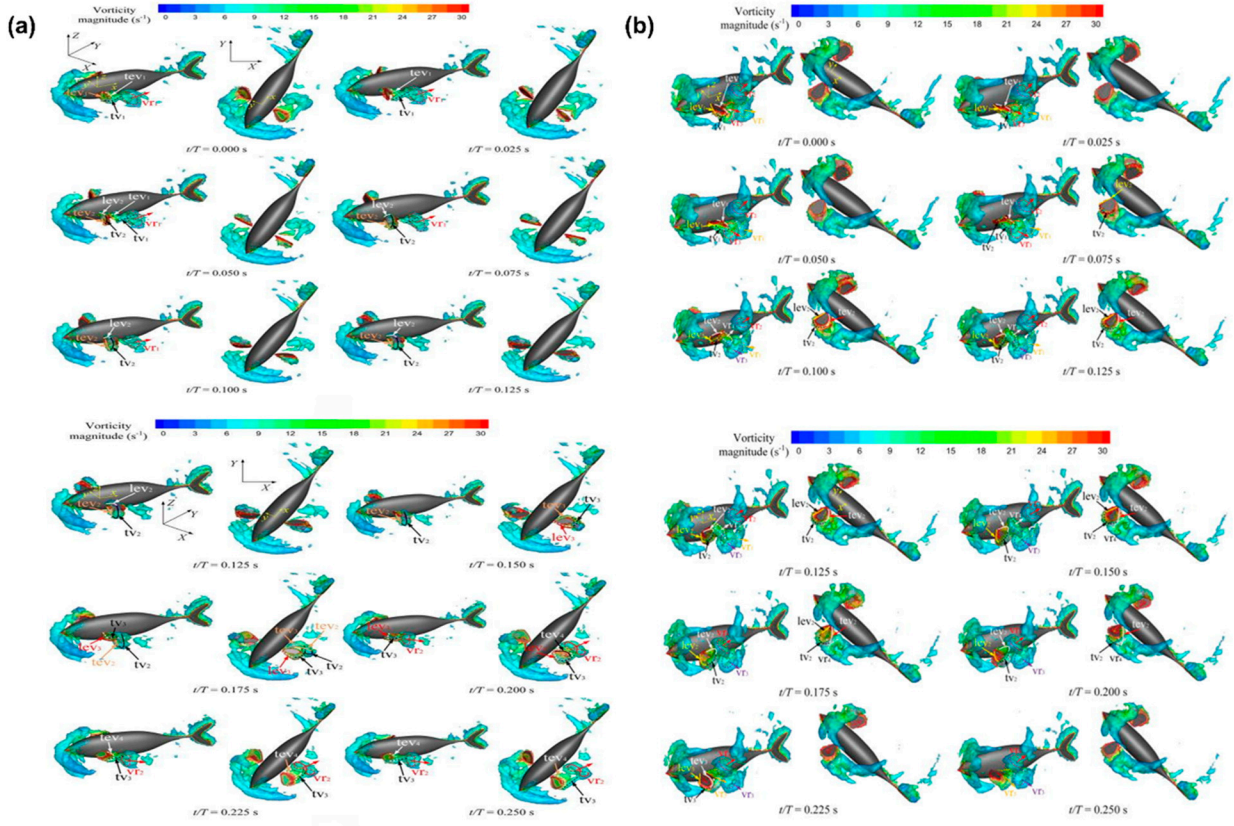

Figure 5: Maneuverability and flow instability utilization in biomimetic propulsion. (**a**,**b**) Adapted with permission from reference [28].

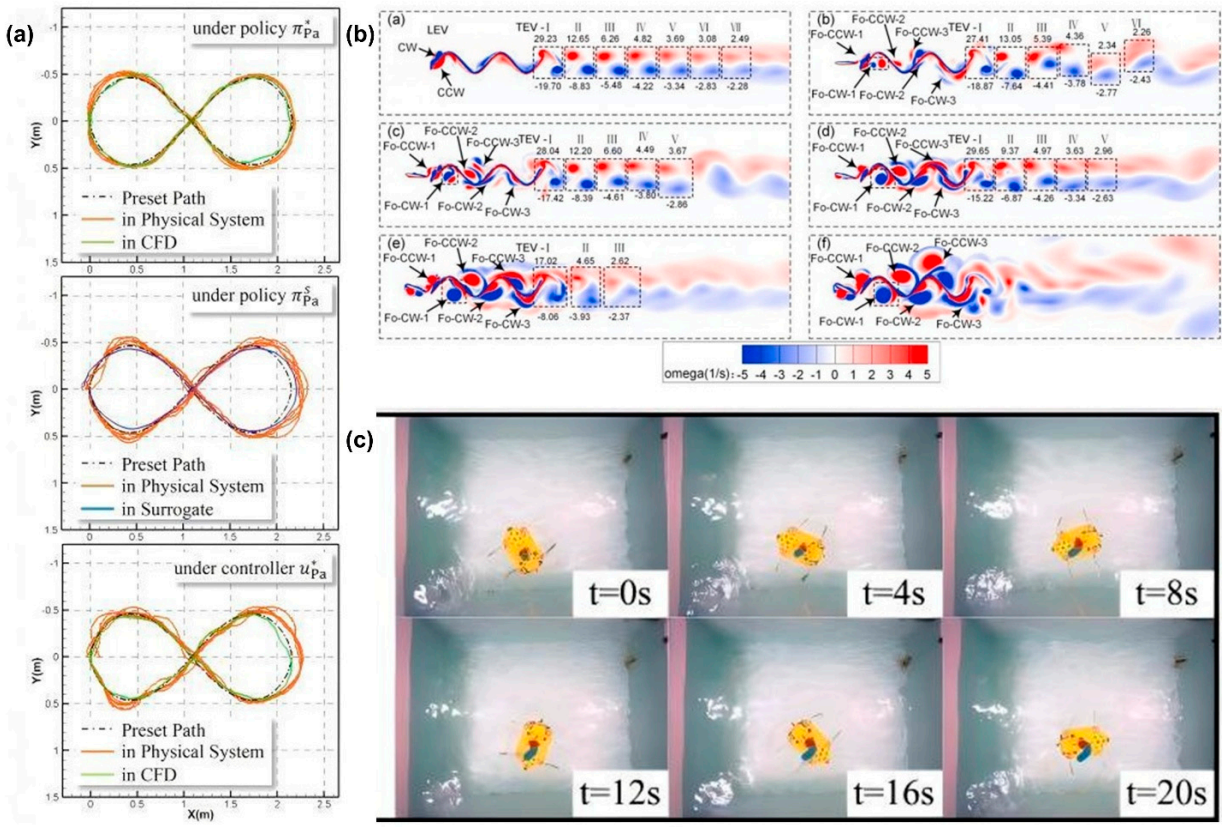

Figure 6: Maneuvering performance and wake interactions in biomimetic underwater vehicles. (**a**) Rapid yaw maneuver of a flexible biomimetic vehicle. (**b**) Wake interaction between tandem or schooling-inspired propulsors. (**c**) Target maneuvering of a fish-like robot under learning-based control. Panels (**a**–**c**) are adapted with permission from Refs. [14,34,62], respectively.

3.4 Biomimetic Drag Reduction and Flow Control

Alongside the pursuit of high-speed and high-efficiency propulsion, minimizing hydrodynamic drag and suppressing deleterious flow perturbations are primary objectives [18,66]. Biological evolution has yielded a variety of sophisticated strategies for drag reduction and flow control, such as the aforementioned dermal microstructures and compliant surfaces [18,68,69]. Additionally, certain species exhibit active control over the flow field near their body surfaces [79,88]. For instance, tuna can erect dermal spinules during high-speed swimming to perturb the boundary layer and delay flow separation [79,88]. Similarly, catfish secrete mucus to lubricate their surfaces, thereby reducing viscous skin friction [89,90]. Inspired by these biological phenomena, research in underwater robotics has extensively explored biomimetic drag-reducing surfaces [18,19,65,66]. A state-of-the-art review by Zhang et al. (2025) summarizes various underwater biomimetic structural and surface technologies, including shark-skin-inspired micro-grooves (riblets), fish-scale-like elastic overlays, superhydrophobic air-retention surfaces, and flexible walls. While these technologies have demonstrated measurable drag reduction effects on a laboratory scale, their practical application still faces numerous challenges [18,19,66,91]. For example, sharkskin-like ribbed plates achieved a surface friction drag reduction of approximately 5%–8% in turbulent water tunnel experiments. However, this effect is limited and requires extremely high manufacturing precision [66,69]. Superhydrophobic surfaces can maintain a stable air film (air layer) in still water, thereby minimizing the wetted area [19].

However, under high pressure and high-speed conditions, this air layer is prone to collapse, limiting its long-term application in deep-sea environments [19,91]. To overcome these challenges and replicate biological efficiency, researchers have developed a variety of advanced biomimetic surface modification techniques, including microribs and superhydrophobic textures, the structural details and drag reduction mechanisms of which are shown in Fig. 7.

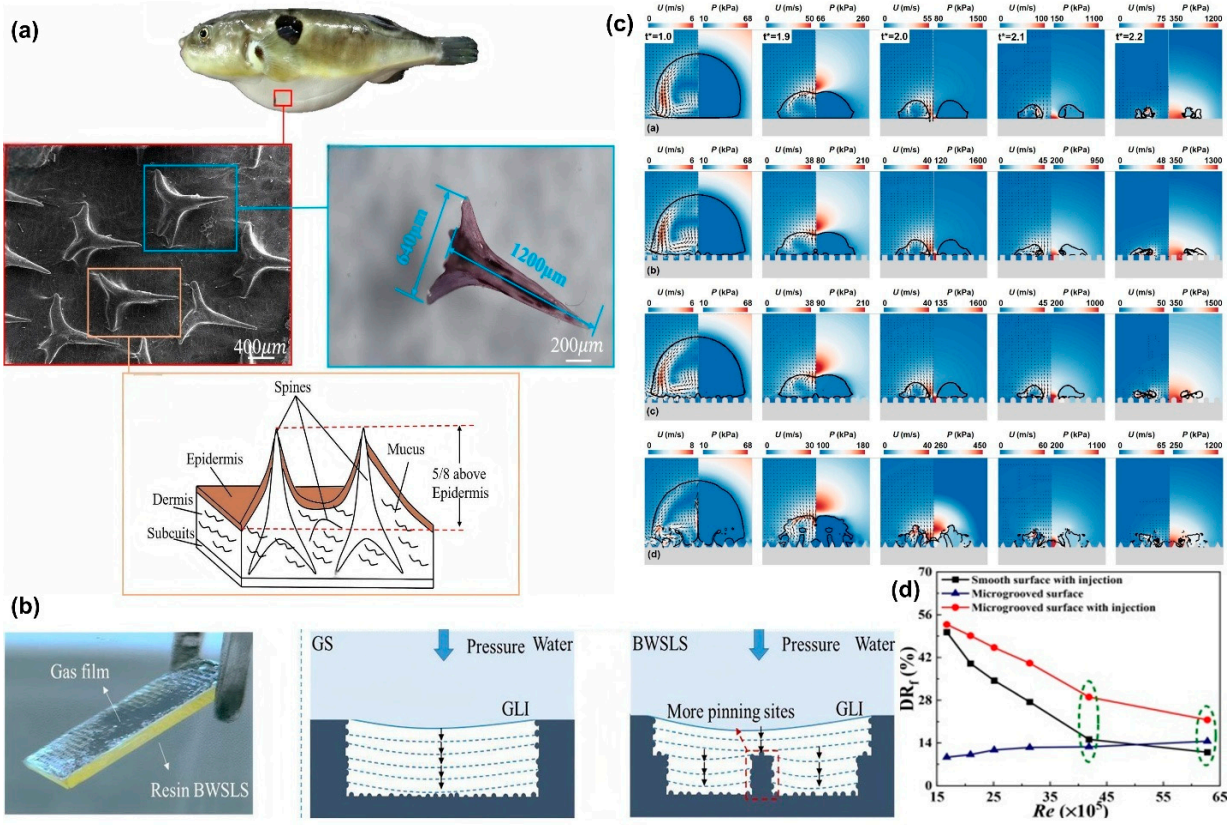

Figure 7: Mechanisms and performance of biomimetic drag-reducing surfaces. (**a**) Pufferfish-inspired micro-spine structures observed by SEM. (**b**) Superhydrophobic surface inspired by butterfly wing scales with stable underwater plastron retention. (**c**) Cavitation bubble collapse regulated by bio-inspired surface textures. (**d**) Drag-reduction rate of a biomimetic superhydrophobic surface under different Reynolds numbers. Panels (**a**–**d**) are adapted with permission from Refs. [19,65,92,93], respectively.

Recently, researchers developed pufferfish-inspired spinule surfaces featuring arrays of divergent micro-spines [76]. PIV observations indicate that these spinules induce a high density of longitudinal vortices in the near-wall region. This promotes the mixing of high- and low-velocity flows, thereby weakening the impingement of the primary inertial vortices on the wall [76]. Zhu et al. (2024) applied these "divergent spinules" to test specimens and observed a 10.48% reduction in friction drag compared to a smooth plate in turbulent boundary layer experiments [76]. PIV and Proper Orthogonal Decomposition (POD) analyses reveal that the spinule surface reduces the correlation scale of turbulent eddies within the boundary layer. Energy is dissipated across smaller-scale vortices, which subsequently diminishes the frictional shear stress acting on the wall. Furthermore, Shi et al. (2024) investigated the impact of biomimetic surfaces on cavitating flows [93]. In high-speed propulsion, conventional rigid propellers suffer from cavitation shedding, which induces vibration and noise [66]. The application of biomimetic micro-textures or coatings

alters the dynamic behavior of cavitation bubbles near the surface, delaying collapse and reducing the resulting impact pressure [93]. Overall, biomimetic drag reduction and flow control technologies hold immense promise for underwater robotic applications [18,66]. However, it must be noted that specific biomimetic surfaces are often effective only under particular operating conditions, exhibiting significant parametric sensitivity [18,19,66]. Future research should pivot toward smart, tunable surfaces—for instance, developing materials that can adjust their roughness or compliance based on real-time flow feedback to achieve adaptive optimization across varying speeds and depths [18,66,94]. It is crucial to emphasize that drag reduction research often involves diverse geometric carriers and evaluation metrics [18,66].

In summary, this section has examined several pivotal aspects of unsteady hydrodynamics [8,18,66]. It is evident that bio-inspired propulsion achieves superior thrust and high efficiency—phenomena largely inexplicable by conventional steady-state theory-through the strategic exploitation of vortex dynamics and unsteady added-mass effects [8]. Concurrently, bio-inspired drag reduction and flow control strategies offer novel paradigms for mitigating hydrodynamic resistance and acoustic signatures [18,66]. These hydrodynamic mechanisms and strategies provide the theoretical foundation for the design and control of underwater bio-inspired robots [8,18,66]. However, their full-scale engineering implementation necessitates further investigation into fluid-structure energy coupling and the role of advanced materials within flexible architectures, which constitutes the focus of the subsequent section [17,93]. The following discussion delves into the FSI mechanisms and energy utilization pathways of flexible propulsive structures [17,93].

4 FSI of Flexible Propulsion and Energy Efficiency

Flexible mechanisms are instrumental to bio-inspired underwater propulsion. Unlike conventional rigid propellers, the fins and tails of bio-inspired robotic fish are typically composed of compliant or elastomeric materials. These structures undergo large-scale deformations during the propulsive cycle, thereby inducing intricate fluid-structure interaction [2,14,16]. This section examines these phenomena through four primary lenses: theoretical modeling strategies, passive morphing mechanisms, the parametric influence of structural flexibility, and energy utilization efficiency.

4.1 Modeling Frameworks for Flexible Propulsion Structures

Accurate simulation of the coupled dynamics between flexible fins and the surrounding fluid is fundamental to elucidating the underlying mechanisms. Classical analytical models include Lighthill's Elongated Body Theory (EBT) for estimating reaction forces on slender bodies, and two-dimensional unsteady airfoil theories for small-amplitude oscillations (e.g., Theodorsen's and Wu's theories) [95–97]. While providing qualitative insights, these theories are constrained by strict assumptions (e.g., small amplitudes and low angles of attack) and thus fail to capture the large-scale flexible deformations inherent in realistic biological propulsion [95–97]. In recent years, researchers have developed various high-fidelity numerical methods to simulate flexible fin propulsion. Representative approaches include:

- Computational Fluid Dynamics with FSI (CFD-FSI): This method directly solves the flow field using the Navier-Stokes equations while simultaneously utilizing elastic dynamics to calculate the structural response. The two domains are coupled through interfacial forces and displacement boundary conditions. For example, the Arbitrary Lagrangian–Eulerian (ALE) method has been used to discretize the tail fin as an elastic body interacting with the surrounding fluid mesh, iteratively updating stress-deformation and flow field at each time step. Although this method offers high accuracy, it is computationally expensive and therefore primarily suitable for validating single-condition applications [14,15].

- Hybrid Immersed Boundary-Lattice Boltzmann Method (IB-LBM): This emerging and efficient technique treats the structure as a boundary immersed in an Eulerian mesh. LBM solves the microscopic fluid dynamic equations, while the immersed boundary applies force feedback based on the structural motion. Qin et al. (2025) developed a solver combining IB-LBM with the Absolute Nodal Coordinate Formulation (ANCF) to achieve high-resolution simulations of large deformations of flexible fins and associated flow fields. ANCF uses the finite element method to describe the large deflection elastic deformation of fins, while LBM effectively captures vortex evolution. This method significantly reduces computational costs while maintaining accuracy, thus facilitating simulation-based parameter optimization [17,20].
- Simplified Multi-Body and Vortex Dynamics Models: To accelerate design iterations, some studies approximate the flexible fish body using articulated multi-segment rigid bodies (often connected via springs) combined with vortex particle or panel methods for flow simulation. For example, a flexible fin can be modeled as a series of rigid plates where bending stiffness is simulated by torsional springs. The hydrodynamic forces on each segment are calculated using quasi-steady airfoil theory or the vortex lattice method. The Pseudo-Rigid-Body Model (PRBM) constructed by Hu et al. falls into this category; by adjusting joint spring stiffness, it accurately reproduces the bending morphology and thrust of flexible fins. These models are computationally efficient and easily integrated into robotic control simulations; however, they require parameter pre-calibration, and their accuracy relies heavily on supporting experimental data [98–100]. Based on the above discussion, Table 2 summarizes the main advantages, limitations, and suitable application scenarios of representative modeling frameworks for flexible bio-inspired propulsion. This comparison shows that no single model is universally optimal: high-fidelity CFD-FSI methods are more suitable for mechanism analysis and validation, whereas reduced-order models are more suitable for rapid design iteration and control-oriented simulation. Among these methods, coupled IB-LBM and ANCF frameworks are particularly useful for resolving large deformation and vortex–structure interaction in flexible fins. Representative numerical frameworks and simulation results are shown in Figs. 8 and 9.

Table 2: Comparison of modeling frameworks for flexible bio-inspired propulsion.

Modeling Framework	Advantages	Limitations	Suitable Applications
ALE-based CFD-FSI	High fidelity; Full flow; Direct coupling	High cost; Mesh issue; Hard convergence	High-fidelity vortex–FSI analysis
IB-LBM	Simple boundary; Moving body; Easy coupling	Grid dependence; Limited high-Re Turbulence challenge	Parametric wake–fin interaction
ANCF-based structural model	Large deformation; Large rotation; High accuracy	Parameter sensitive; Solver coupling; Added cost	Large-deformation fin mechanics
Reduced-order/PRBM models	Fast solving; Easy control; Low cost	Lower fidelity; Calibration needed; Limited flow details	Soft-actuator design

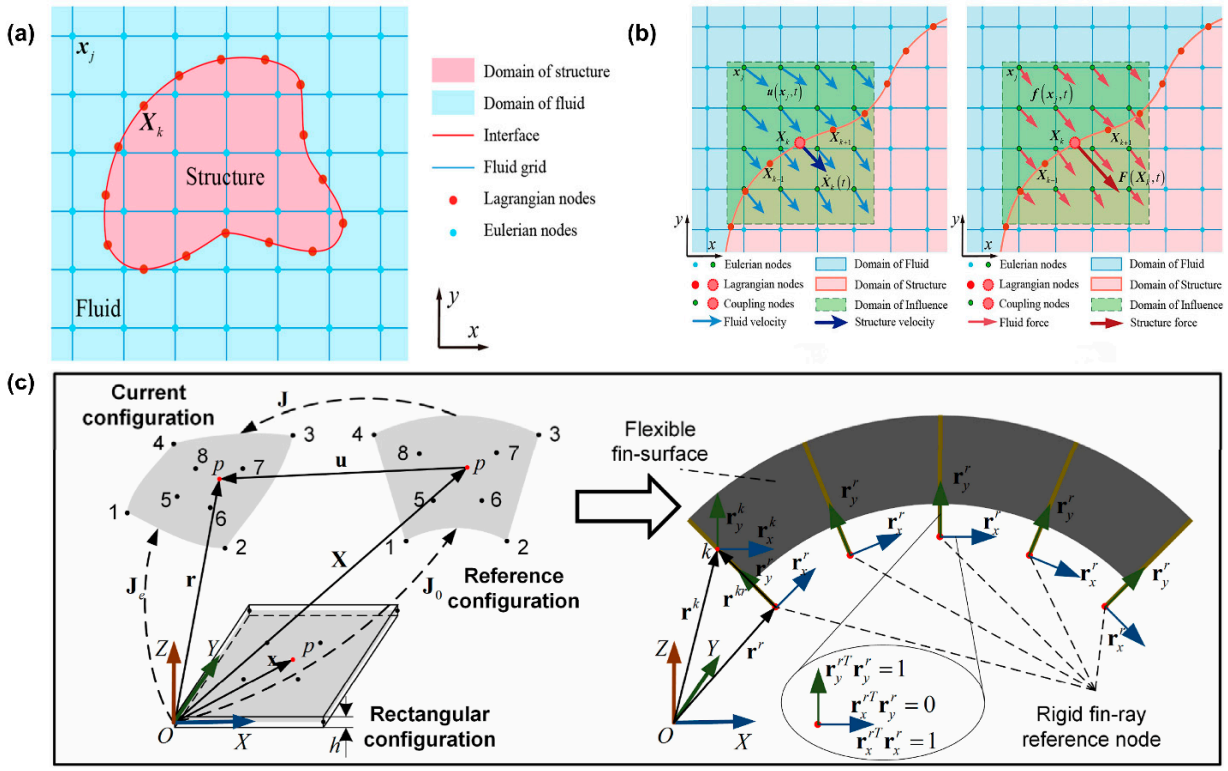

Figure 8: Numerical frameworks and simulation strategies for flexible FSI. (**a**,**b**) Immersed-boundary lattice Boltzmann framework for FSI simulation with fixed fluid grids and moving structural boundaries. (**c**) Absolute nodal coordinate formulation for large-deformation modeling of flexible fin structures. Panels (**a**–**c**) are adapted with permission from Refs. [17,27,101], respectively.

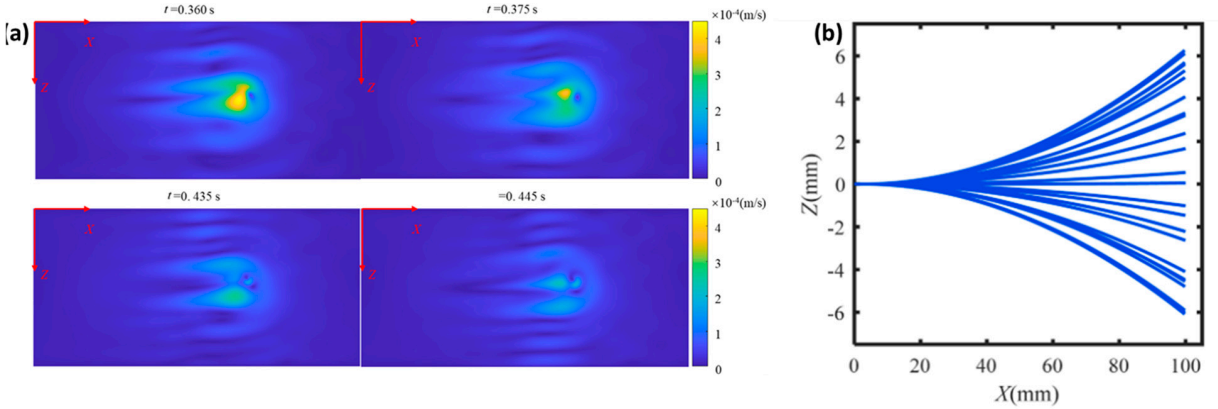

Figure 9: FSI simulation results demonstrating the macroscopic structural and fluidic responses. (**a**) the overall large deformation envelope of a flexible biomimetic fin during actuation. Adapted with permission from reference [20]. (**b**) The corresponding flow field velocity distribution, accurately captured via the coupled ANCF-IB-LBM framework. Adapted with permission from reference [20].

Regardless of the modeling approach, it is essential to validate its fidelity in reproducing the underlying physical phenomena. Bai et al. (2022) designed a flexible biomimetic fish fin made of an elastic rubber material and developed a coupled hydrodynamic–structural model; by acquiring response data from free-

vibration and forced-vibration experiments, they successfully identified the model parameters. Similarly, Zeng et al. (2025) used a self-developed undulating-wing experimental platform to measure transient fin deformation and thrust at different frequencies, thereby validating the accuracy of their CFD + elastic-beam model [14,16,20]. By coupling the flexible-fin dynamic equation with the Navier–Stokes equations, or by adopting an empirical hydrodynamic model, one can solve for the fin response and the resulting thrust under prescribed actuation conditions [17,20,53]. Contemporary research in bio-inspired robotics is increasingly moving toward hybrid paradigms that integrate data-driven approaches with physics-based models to improve predictive accuracy and computational efficiency. For example, high-fidelity CFD results can be used to learn unknown force terms in reduced-order models, or to update flexible-fin model parameters online so that the model remains valid across the full operating envelope [99,102]. In summary, establishing a reliable and efficient modeling framework for flexible propulsion is a prerequisite for subsequent design optimization and control. Existing models still exhibit limitations in accounting for turbulent effects and three-dimensional fin geometries, and further advances are required to encompass more complex, realistic operating conditions [16,17,20].

4.2 Coupling Mechanisms between Passive Deformation and Active Actuation

During oscillation, flexible propulsors typically receive energy input from active actuation (e.g., motors or smart actuators); however, their morphological evolution is governed by passive elastic deformation. The coupling of these two factors yields a unique dynamic response [14,16,53]. Fundamentally, the flexible fin does not strictly follow the kinematic trajectory of the driving signal. Instead, it undergoes secondary motion induced by hydrodynamic forces acting upon its intrinsic elasticity. This process can introduce phase lags, filter high-frequency components, or even trigger resonant amplification effects [53,56,103]. This passive deformation is often termed "compliance." Appropriate compliance can enhance propulsion efficiency by effectively yielding to fluid forces; conversely, excessive compliance may result in power loss [103–105]. The underlying mechanisms are elucidated below through representative phenomena:

- Thrust Vector Alignment Effect: As mentioned earlier, the flexible fins maintain their inertia in the original direction of motion due to deformation during stroke reversal, thus avoiding abrupt changes in the thrust vector. Passive deformation causes the fin surface angle to lag behind the instantaneous direction of motion, effectively reducing the angle of attack and mitigating negative thrust [56,104]. This effect is similar to the damping mechanism of a kite tail, acting as a rectifier in the propulsion cycle. For example, experiments comparing flexible tail fins with rigid plates of equal length show that flexible tail fins exhibit significant bending at the end of the stroke. This makes the wake vortex shedding angle closer to the axial direction, thereby increasing the effective thrust by approximately 30%.
- Energy Storage and Release: Flexible materials can store a portion of the driving energy in the form of strain energy and release it into the fluid at appropriate stages. Specifically, at the beginning of the stroke, some of the input work is used to bend the fins and is temporarily stored within the structure. As the fins cross the centerline and begin to decelerate, the elastic rebound of the structure feeds this energy back into the fluid, accelerating wake vortex shedding and jet formation. Therefore, flexible fins can recover kinetic energy that would otherwise be dissipated [53,103]. This mechanism is particularly significant under resonant conditions: when the driving frequency is close to the natural frequency of the fin, the amplitude increases significantly, and the elastic deformation period is synchronized with the driving frequency, thereby achieving efficient reciprocating energy conversion. Lucas et al. (2015) demonstrated that higher propulsion speeds can be obtained by changing the stiffness distribution to

match the natural frequency of the fin with the driving frequency [103]. This shows that adjusting the passive flexibility parameters to induce near-resonant behavior can significantly improve propulsion performance [53,103].

- Coupled Phase Optimization: A relative phase shift exists between the active actuation (e.g., periodic motor torque) and the passive fin response. This phase determines the timing of strain energy release to the fluid. To maximize thrust, the ideal scenario requires the fin tip deformation to peak exactly when displacing the maximum volume of water, ensuring that thrust generation is in phase with velocity [104]. By selecting appropriate materials and driving frequencies, the relative phase between structural and hydrodynamic forces can be optimized. Conversely, an improper phase difference—such as the fin bending to absorb energy during the peak thrust generation window—will attenuate net thrust. Simulation studies by Miao et al. indicate that the thrust-displacement phase diagrams vary with fin flexibility. Moderate flexibility yields an ideal counter-clockwise loop (indicating positive work output), whereas excessively rigid or soft fins increase the clockwise area (indicating energy dissipation). Thus, a set of optimal flexibility parameters exists that synchronizes the active-passive coupling phase, thereby maximizing thrust and efficiency [104,106,107]. The fundamental mechanisms of this active-passive coupling, including the optimization of passive deformation envelopes and the phase synchronization required for effective strain energy storage and release, are conceptually detailed in Figs. 10 and 11.

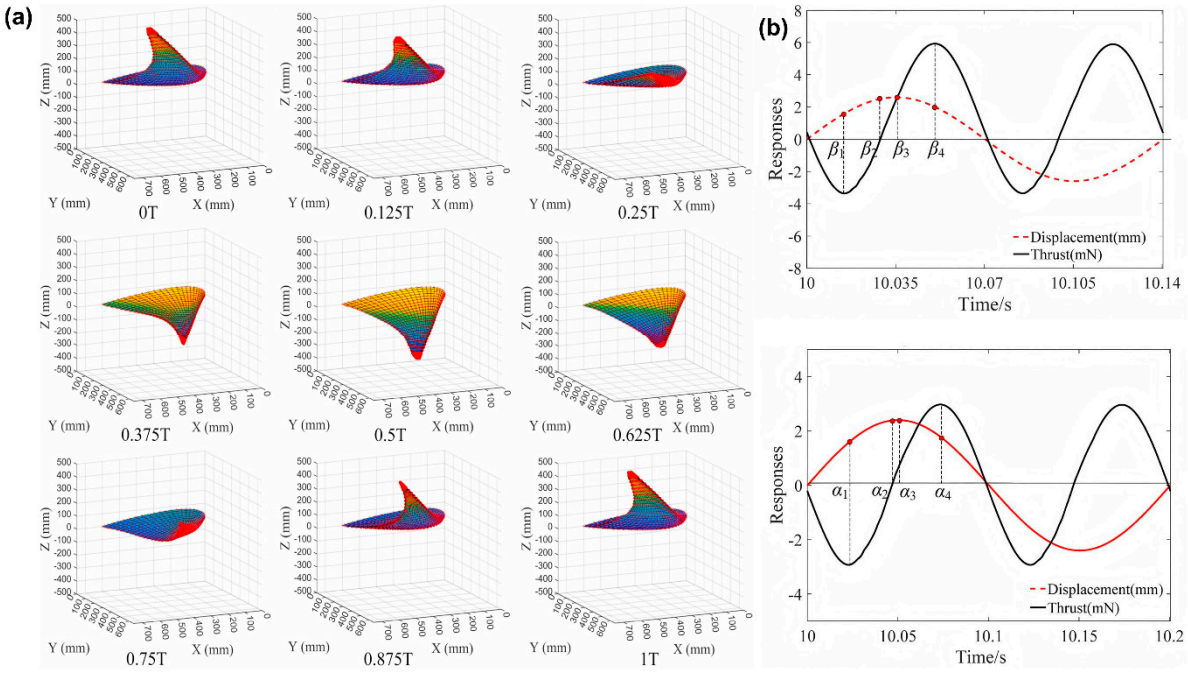

Figure 10: Passive deformation mechanics and thrust generation in flexible propulsors. (**a**) Time-lapse simulation of biomimetic fin deformation during one oscillation cycle. (**b**) Phase-coupled displacement and thrust responses associated with elastic energy storage and release. Panels (**a**,**b**) are adapted with permission from Refs. [27,101], respectively.

It must be noted that excessive passive compliance can have adverse side effects: fins may bend excessively, leading to a significant reduction in the effective angle of attack, or even reverse bending, thereby weakening thrust [56,105]. Experimental evidence shows that while overly soft fins can reduce vortex

interference, their thrust is lower than that of a rigid baseline [56,105]. This indicates that flexibility requires a trade-off under a fixed active drive input. To address this issue, advanced biomimetic design introduces the concept of semi-active control, utilizing variable stiffness materials (such as shape memory polymers) to construct fins. This allows the compliance of the fins to be adjusted in real time to adapt to different speed and maneuver requirements [106–108]. This strategy of "active control of passive deformation" promises to combine the advantages of both approaches: relaxing the fins to enhance compliance during efficient cruise and increasing their stiffness to boost thrust during sprint maneuvers [106–108]. In summary, the ingenious combination of active drive and passive deformation enables biomimetic thrusters to simultaneously function as energy absorbers (buffers) and energy releasers (thrusters). This remains one of the fundamental mysteries behind the high-speed and efficient swimming of aquatic organisms [103,104].

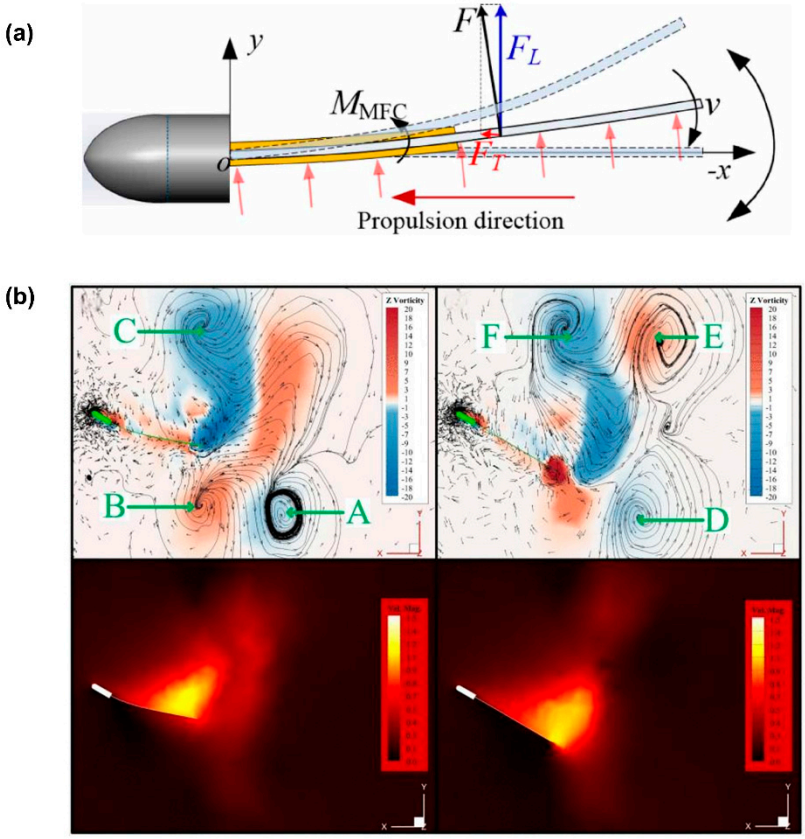

Figure 11: Thrust vector alignment in flexible propulsive structures. (**a**) Schematic illustration of thrust-vector alignment. (**b**) CFD validation of thrust-vector alignment. Passive flexibility reorients local hydrodynamic forces and increases the thrust-direction force component during flapping. Panels (**a**,**b**) are adapted with permission from Refs. [14,101], respectively.

4.3 Influence of Flexibility Parameters on Propulsion Performance and Maneuverability

The performance of flexible propulsors is intrinsically contingent upon their material and geometric parameters, including stiffness distribution, mass distribution, damping characteristics, and three-dimensional morphology [16]. Variations in these parameter combinations lead to significant alterations in propulsion efficiency, thrust coefficients, and maneuvering agility [16,109]. Key influence laws derived from comparative studies are elucidated below. To facilitate the comparison of evaluation metrics and configuration differences

among various flexible designs, the following part summarizes typical configurations of jointed/flexible caudal fin systems, the definition of the TPR metric, and the explanatory framework for thrust-vectoring.

- Flexural Rigidity: Stiffness governs the deformability of the fin. Generally, fins with intermediate flexibility exhibit superior efficiency and thrust compared to rigid counterparts [15,109,110]. However, performance degrades if the fin is excessively soft, indicating the existence of an optimal stiffness range [15,109,110]. Shinde et al. (2014) varied the thickness of flexible caudal fins and observed that as flexural rigidity (EI) increased from 10^{-7} Nm^2, thrust followed a non-monotonic trend (increasing then decreasing) [77,109,110]. At excessively low stiffness, the fin suffers from severe kinematic lag, resulting in insufficient thrust amplitude. Conversely, at excessively high stiffness, the fin undergoes negligible deformation, failing to exploit compliance benefits and causing strong vortex interference [109,110]. Under optimal stiffness, the fin deformation is moderated, maximizing both thrust and efficiency [15, 109,110]. For instance, Lucas et al. implemented a gradient stiffness profile (stiff root, compliant tip) in a bio-inspired fin, achieving a swimming speed approximately 20% higher than that of a uniform-stiffness fin [111,112]. Therefore, optimizing fin stiffness for target speeds is critical in design [15,110]. Consequently, understanding the parametric sensitivity of propulsive performance to structural variables such as flexural rigidity profiles and three-dimensional fin morphology is paramount, as quantitatively demonstrated in Fig. 12.
- Mass and Flexibility Distribution: The mass distribution of the fin dictates its inertial characteristics and mode shapes. Increasing tip mass reduces the natural frequency and amplifies deformation amplitude, potentially enhancing low-frequency thrust but causing excessive lag at high frequencies [109,113]. Reddy et al. (2018) concluded that uniform flexibility is not necessarily optimal; rather, distributed flexibility enhances performance [109,112]. For example, Lucas et al. demonstrated that stiffening the anterior 1/3 of the fin while keeping the posterior 2/3 flexible results in both large oscillation amplitudes and sufficient caudal rigidity, thereby maximizing thrust [111,112]. This suggests that tuning the flexibility distribution (e.g., stiff-anterior/soft-posterior, or soft-middle/stiff-ends) can optimize morphing kinematics to maximize propulsion. Notably, requirements for flexibility distribution vary by swimming mode: BCF caudal fins typically feature a stiff base and a compliant tip, whereas MPF types (e.g., ray pectoral fins) require overall flexibility to propagate propulsive waves.
- Three-Dimensional Morphology and Torsional Compliance: Real fish fins are complex 3D membrane structures capable of both bending and twisting. Torsional compliance allows for adaptive variations in the angle of attack during flapping. Experiments indicate that fins with torsional compliance automatically adjust their angle of attack during upstrokes and downstrokes, symmetrizing thrust generation across the two half-cycles and reducing thrust fluctuation. Young et al. (2020) reported that adding a small hinged flap to the trailing edge of a rigid fin—effectively imparting passive torsional flexibility—resulted in more regular wake vortices and a ~15% efficiency increase [60]. Thus, rational 3D flexibility (bending + torsion) facilitates the favorable distribution of fluid forces and improves performance [27,114].
- Damping: Internal material damping and external hydrodynamic damping serve to dissipate vibrational energy [113]. In bio-inspired fin design, moderate damping is generally desired. Insufficient damping can lead to excessively sharp resonance peaks and uncontrollable dynamic responses, while excessive damping absorbs valuable strain energy, reducing efficiency [113]. It is often observed that the quality factor (Q-factor) of flexible fins is lower in water than in air due to significant hydrodynamic radiation damping [113]. Chen et al. noted that appropriate structural damping suppresses high-order harmonics at the fin tip, thereby maintaining coherent vortex formation, whereas excessive damping diminishes

elastic energy storage effects. Consequently, damping must be co-optimized with stiffness and driving frequency [16,113].

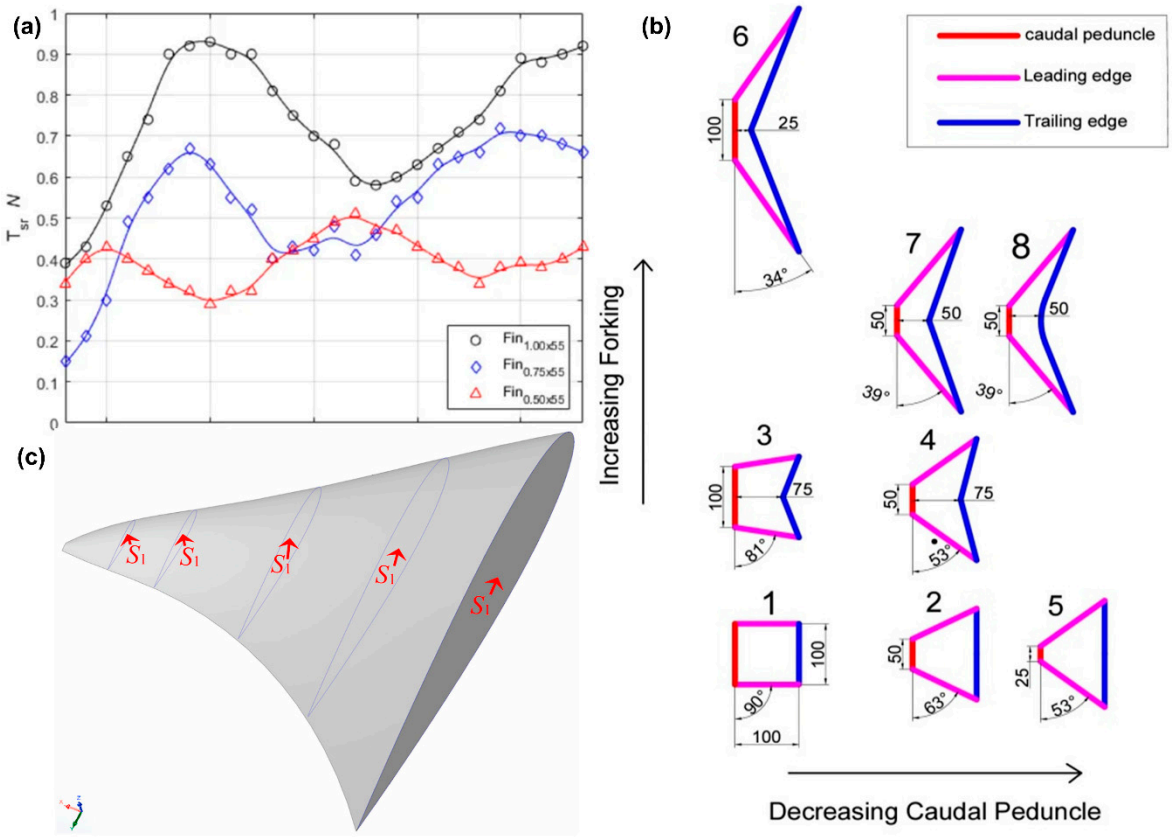

Figure 12: Structural parameters affecting hydrodynamic performance. (**a**) Mean thrust variation with fin length and thickness. (**b**) Parametric caudal-fin morphologies for efficiency optimization. (**c**) Variable-stiffness biomimetic fin based on a multilayer laminate structure. Panels (**a**–**c**) are adapted with permission from Refs. [20,54,110], respectively.

In summary, the performance of flexible propulsors exhibits high parametric sensitivity. Optimal designs typically require identification through extensive simulation and experimental parameter sweeps tailored to specific applications [16,109]. For example, Zeng et al. (2025) systematically analyzed the thrust and efficiency distributions of wave-shaped fins under different flexibility-frequency combinations using numerical simulations, creating a "performance map" to guide optimization [16]. Future research could leverage machine learning algorithms to efficiently explore the vast parameter space and identify the optimal flexible configuration that simultaneously meets the requirements of high-speed cruise and agile maneuverability.

4.4 Energy Transfer Pathways and Propulsion Efficiency Analysis

Clarifying the energy utilization mechanisms in flexible biomimetic propulsion systems is crucial for improving efficiency [14,16,47,115]. Unlike rigid propellers that directly convert shaft power into thrust, energy in flexible propulsion systems undergoes a series of conversions and distribution processes [14,16,26,47]. Mechanical energy provided by actuators (e.g., motors) is transferred to the fins via linkages or chords [47,115]. Part of this energy is converted into the kinetic and strain energy of the fins, and then

transferred to the wake vortex to generate thrust by doing work on the fluid [14,16,47,115]. The remaining energy is dissipated as vortex ring kinetic energy or thermal energy [23,113,115].

To quantitatively assess propulsion performance, the Froude propulsive efficiency is commonly defined as the ratio between the cycle-averaged useful propulsive power and the cycle-averaged input power:

$$\eta_F = \frac{\overline{P}_{\text{prop}}}{\overline{P}_{\text{in}}} = \frac{\overline{T}U}{\overline{P}_{\text{in}}}, \tag{1}$$

where $\overline{T}$ is the cycle-averaged thrust, U is the swimming or incoming-flow velocity, $\overline{P}_{\text{prop}} = \overline{T}U$ is the useful propulsive power, and $\overline{P}_{\text{in}}$ is the cycle-averaged input power supplied by the actuator or prescribed motion. For motor-driven robotic systems, the input power can be estimated from actuator torque and angular velocity as

$$\overline{P}_{\text{in}} = \frac{1}{T_c}\int_0^{T_c} \tau(t)\omega(t)\,\mathrm{d}t, \tag{2}$$

where T_c is one flapping period, $\tau(t)$ is the actuator torque, and $\omega(t)$ is the angular velocity. For multi-actuator systems, the term $\tau(t)\omega(t)$ can be replaced by the summation of the instantaneous power of all actuators. In numerical FSI studies or prescribed-motion simulations, the input power may alternatively be calculated from the rate of work associated with hydrodynamic loading on the moving or deforming propulsor surface:

$$\overline{P}_{\text{in}} = \frac{1}{T_c}\int_0^{T_c}\int_S \mathbf{f}_h(\mathbf{x},t)\cdot\mathbf{u}_s(\mathbf{x},t)\,\mathrm{d}S\,\mathrm{d}t, \tag{3}$$

where S is the propulsor surface, $\mathbf{f}_h(\mathbf{x},t)$ is the hydrodynamic force density, and $\mathbf{u}_s(\mathbf{x},t)$ is the local surface velocity. The sign convention should be chosen consistently so that positive input power denotes energy supplied to the fluid–structure system.

Other commonly used metrics include the thrust-to-power ratio (TPR) and the cost of transport (CoT):

$$\text{TPR} = \frac{\overline{T}}{\overline{P}_{\text{in}}},\ \text{CoT}_m = \frac{\overline{P}_{\text{in}}}{mU},\ \text{CoT}_w = \frac{\overline{P}_{\text{in}}}{mgU}, \tag{4}$$

where m is the robot mass and g is gravitational acceleration. CoT_m denotes the mass-normalized energy cost per unit distance, whereas CoT_w is the weight-normalized form commonly used for cross-system comparison. Therefore, efficiency values reported in different studies should be compared only when the same metric definition, measurement boundary, Reynolds number, Strouhal number, actuation protocol, and testing condition are used [23,116]. The efficiency bottleneck of flexible propulsion stems from the incomplete release of strain energy stored within the structure in each cycle, as well as energy dissipation caused by parasitic vortex formation, turbulence, and internal material damping [23,113,117]. Fig. 13 compares the thrust-to-power ratio of representative propulsor designs and illustrates the effects of frequency and actuation parameters on net thrust and propulsion efficiency.

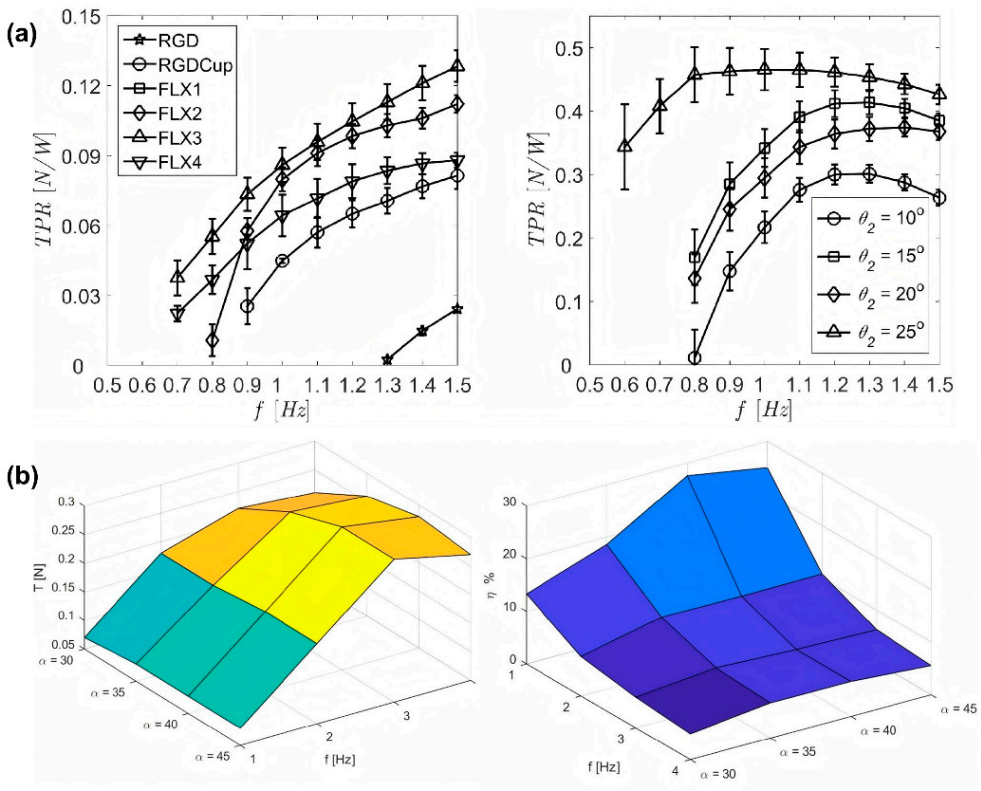

Figure 13: Energy efficiency and performance trade-offs in biomimetic propulsion. (**a**) Thrust-to-power ratio comparison among different propulsor designs. (**b**) Three-dimensional performance maps showing the effects of frequency and angle on net thrust and efficiency. Panels (**a**,**b**) are adapted with permission from Refs. [56,118], respectively.

Recent experimental studies have quantified the overall efficiency of robotic fish under various operating conditions and analyzed the energy budget [16,84]. For instance, Badu et al. (2020) reviewed efficiency data for flapping wing systems, noting that single flexible foils typically exhibit efficiencies in the 50–70% range, significantly outperforming equivalent small-scale propeller systems (30–50%) [84]. Dual-foil coupled propulsion can further elevate efficiency to exceed 70% under optimized phase conditions [84,119]. To dissect energy pathways, researchers draw upon power decomposition methodologies from aerodynamics, separating propulsion power into useful work and various loss components [116,120]. Blake et al. (2004) proposed categorizing fish swimming expenditures into induced power (required to accelerate the wake), frictional power (viscous dissipation), and recoil power (inertial losses due to body oscillation) [120]. Structural compliance mitigates recoil inertial losses because the flexible body avoids accelerating the entire water mass in ineffective reciprocating motion, instead channeling more motion into useful vortex momentum output [120,121]. Furthermore, the introduction of elastic energy storage-and-release mechanisms facilitates the partial recovery of inertial energy [113,117]. Wainwright et al. demonstrated via numerical simulations that flexible fins incur significantly lower energy losses per cycle compared to rigid paddles. Especially at higher frequencies, flexible fins convert energy—which would otherwise be wasted by rigid paddles—into useful wake kinetic energy [98,121].

From an energetic perspective, metrics such as the energy consumption per unit thrust (J/N) or energy per unit distance (i.e., Cost of Transport, CoT) are employed to evaluate efficiency [98,116,122]. Biological organisms excel in this regard—slow swimmers like jellyfish demonstrate exceptionally low CoT,

attributed to their ingenious exploitation of vortex ring rebound and elastic storage mechanisms [43,122,123]. To approximate this biological performance, bio-inspired robotic design must explicitly manage energy flux: channeling input energy primarily into thrust-generating pathways while minimizing dissipation channels [14,16,122]. Strategies include: optimizing fin flexibility to resonate with the flapping frequency, thereby maximizing the conversion of actuation energy to vortex kinetic energy [121,124]; minimizing non-propulsive lateral motion and vortices (e.g., using symmetric dual fins to cancel lateral forces) [26,125]; and utilizing high-elasticity, low-damping materials to reduce internal hysteresis [113,117]. A novel concept proposed by Xie et al. (2022) is the "unidirectional fluid transport structure": specially designed microstructures allow fluid flow only in the propulsion direction while blocking reverse flow, potentially reducing backflow losses. Although currently at the material testing stage, this fluidic diode-like concept offers a new avenue for enhancing net energy utilization [126].

Finally, it is worth noting that the high efficiency of flexible biomimetic propulsion systems is often limited to specific speed or frequency ranges. Efficiency can drop significantly when operating outside of the design conditions [16,121,124]. Therefore, maintaining high average efficiency across multiple speed ranges is a challenge. One feasible solution is to employ adaptive regulation: for example, using variable stiffness fins or multimodal thrusters to employ eel-shaped whole-body undulations (high-thrust mode) at low speeds and tuna-shaped hard-tail oscillations (high-efficiency mode) during high-speed cruise, thus maintaining near-optimal efficiency under various conditions. This effectively requires a trade-off between propulsion efficiency and maneuverability [107,127]. In summary, the discussion in this section demonstrates that flexible propulsion structures achieve higher energy utilization efficiency than conventional propulsion systems by regulating active and passive energy flows. However, to fully realize this advantage, precise modeling and optimization of the energy distribution of each branch are needed, representing a key focus for future research and engineering implementation [16,115,127].

5 Role of Deformable Soft Materials and Bio-Inspired Surfaces in Underwater Propulsion

Materials serve as the bridge connecting structural design with the fluid environment. The application of novel deformable soft materials and bio-inspired surfaces is expanding the performance boundaries of bio-inspired underwater robots [1,16,24]. This section summarizes typical flexible propulsion materials and their underwater mechanical properties, recent smart and self-healing material systems, soft robotic actuators and their coupling with fluid loads, and the fluid adaptability of bio-inspired surfaces/soft shells, discussing relevant experimental evidence and limitations [115,128].

First, regarding flexible propulsion materials, polymer materials such as silicone rubber and polyurethane elastomers are commonly used. They possess low Young's modulus and high extensibility, resembling biological tissues [24,129]. For instance, the caudal fins of most robotic fish are cast from silicone with a hardness of approximately Shore A20–50, enabling them to withstand repeated bending without fatigue cracking. These materials exhibit excellent compliance underwater: they deform locally upon fluid impact to buffer loads, thereby reducing peak stresses [16,24,129]. However, purely passive flexible materials have limitations; their response speed is constrained by intrinsic material damping and inertia, preventing rapid shape adjustment [16,24]. Consequently, various smart actuating materials have been developed in recent years, combining actuation and flexibility functions to enable bio-inspired propulsors to be both deformable and actively controllable. Table 3 lists common smart materials and their properties [24,130,131].

Table 3: Comparison of common smart actuating materials for bio-inspired underwater propulsion and their characteristics.

Material Type	Max Strain	Response Frequency	Advantages	Disadvantages
Ionic Polymer-Metal Composite (IPMC) [132]	2%–5%	<5 Hz	Low driving voltage; Soft and flexible; Silent actuation	Low output force; Slow response; Hydration required
Shape Memory Alloy (SMA) [133]	4%–8%	0.1–1 Hz	Large strain; High power density; Muscle-like actuation	Low efficiency; Slow cooling; Thermal hysteresis
Macro Fiber Composite (MFC/PZT) [13]	<0.1%	<20 Hz	Ultra-fast response; high force density; precise actuation	Small strain; High voltage required; Brittle
Dielectric Elastomer (DE) [32]	20%–100%	<200 Hz	Very large strain; Lightweight; High efficiency	High electric field; Pre-stretch required; Durability issues
Magnetostrictive Materials [32]	0.1%–0.2%	<100 Hz	Fast response; High precision; Strong controllability	Small strain; High magnetic field; Bulky system

Moving beyond theoretical potential, Fig. 14 highlights representative implementations of MFC-, IPMC-, and SMA-actuated biomimetic underwater propulsors—in driving the next generation of highly compliant bio-inspired propulsors.

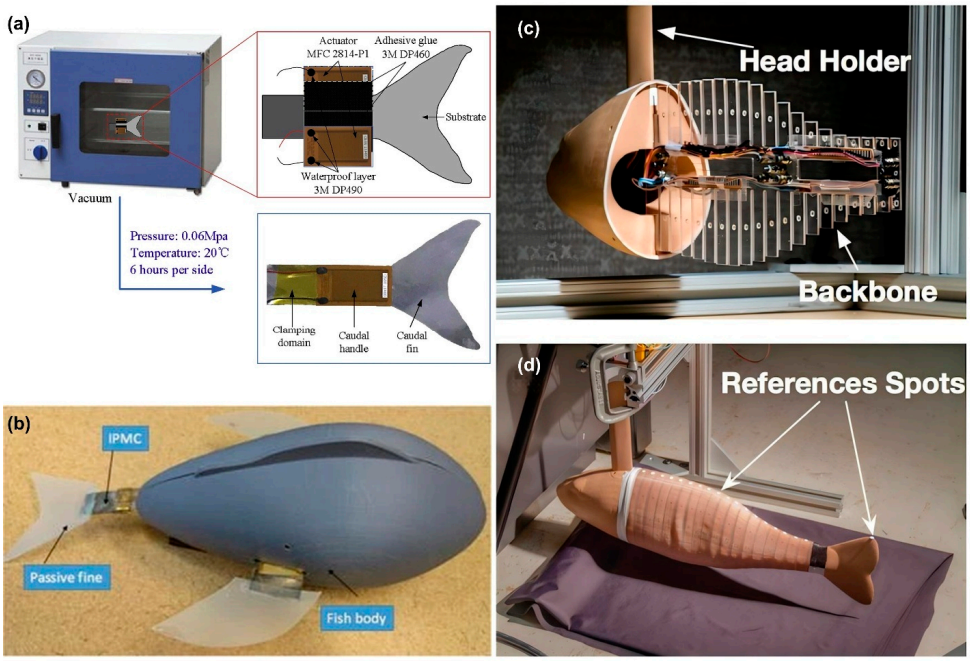

Figure 14: Smart materials and artificial muscles for biomimetic underwater propulsion. (**a**) MFC-actuated biomimetic caudal fin for piezoelectric propulsion. (**b**) IPMC-driven soft robotic fish with flexible fin oscillation. (**c**,**d**) SMA-wire-actuated biomimetic fish based on thermally induced contraction. Panels (**a**–**d**) are adapted with permission from Refs. [13,134,135], respectively.

As detailed in Table 3, each material class exhibits distinct advantages and limitations. Ionic Polymer-Metal Composites (IPMC) offer superior compliance, making them suitable for the oscillation of small robotic fish fins; however, due to limited force generation, they are predominantly employed in pectoral fins with small undulation amplitudes [24,136,137]. Shape Memory Alloys (SMA) provide substantial contraction force suitable for driving stiffer mechanisms (e.g., robotic fish trunk joints), yet their low operating frequency renders them unsuitable for high-speed swimming [24,138]. Piezoelectric Macro Fiber Composites (MFC) are frequently utilized to drive small-scale flapping wings or propulsors [13,24]. For instance, Lou et al. employed MFC patches to drive a micro-caudal fin, achieving precise waveform control and 3D vortex generation [13]. Dielectric Elastomers (DE) (e.g., 3M VHB films) are capable of large strains and have been applied to fabricate jellyfish robot bells, mimicking biological contraction propulsion. However, DE films necessitate effective solutions for waterproofing and high-voltage safety [47,131,139].

Beyond these commonly used smart actuating materials, several emerging material systems are attracting increasing attention for underwater bio-inspired robots. Self-healing elastomers and hydrogels provide a promising route for improving damage tolerance in soft fins, compliant skins, and deformable sealing structures, especially under long-term cyclic bending, abrasion, and accidental contact with complex underwater environments. Liquid crystal elastomers (LCEs) can achieve programmable and reversible shape morphing under thermal, optical, or electrical stimuli, making them suitable for adaptive fin camber control and soft-bodied deformation [130,140]. HASEL-type electrohydraulic actuators and other artificial-muscle-based soft actuators combine large deformation with intrinsic compliance, offering potential advantages for jellyfish-like, squid-like, and fish-like soft robotic platforms. In addition, variable-stiffness composites and fiber-reinforced elastomers enable spatially graded compliance, allowing propulsive structures to remain flexible during energy-efficient cruising while increasing stiffness during rapid acceleration or maneuvering. Nevertheless, these emerging materials still face several engineering challenges, including waterproof encapsulation, response-speed limitations, fatigue under repeated actuation, high-voltage safety in underwater environments, material degradation after long-term immersion, and integration with compact onboard power systems.

In summary, no single material simultaneously optimizes strain, speed, force, and efficiency. Consequently, practical designs often adopt multi-material combinations or structural amplification schemes [24,130,131]. For example, certain robots employ a “motor + flexible transmission” hybrid drive: the motor provides high force, while a flexible coupling introduces compliance to protect the structure and simulate biological softness. Other studies parallel SMAs with springs to form composite actuators, enhancing response frequency while maintaining significant strain [24,130,138]. Regardless of the scheme, the interaction between the material and the fluid is a critical consideration [15,16,115]. First, materials may exhibit different properties in water compared to air (e.g., IPMC demonstrates improved current conduction and heat dissipation in water, tolerating slightly higher frequencies) [136,137]. Second, fluid loads significantly influence material deformation; for instance, the bending morphology of an IPMC fin under hydrodynamic loading differs from that in air [15,136]. Therefore, designs must evaluate the actual underwater output deformation and thrust via FSI simulation or experiments, rather than relying solely on dry-state performance [15,16].

The following discussion turns to biomimetic surfaces and soft shells. Many underwater robots employ soft skins or localized biomimetic coatings to enhance hydrodynamic performance and environmental adaptability [1,24,141]. For example, MIT’s soft robotic fish uses a silicone skin to encase its body, which not only optimizes its shape but also absorbs environmental impacts and reduces flow noise. Biomimetic surfaces, such as the aforementioned sharkskin texture and superhydrophobic coatings, have been experimentally

demonstrated to reduce frictional drag [16,93,128,142]. Xie et al. (2022) developed a unidirectional porous fluid structure (inspired by marine zooplankton) containing directional pores that allow fluid to permeate in one direction while preventing it from flowing in the opposite direction. When applied to a robot surface, forward-generated pressure is released through the pore portions (thus reducing pressure drag), while reverse flow is impeded, which may help improve the robot's stability in wave environments. Although performance data remain limited, this design exemplifies the dynamic adaptability of biomimetic soft surfaces to flow fields [126].

In drag reduction design for engineering applications, the synergistic effect of micro structured surfaces (e.g., microgrooves/ribs) with viscoelastic drag reducers (DRAs) is considered a feasible and scalable approach [142–144]. In addition to frictional drag, biomimetic textures and soft shells can significantly modulate local peak loads and noise source intensity caused by near-wall unsteady phenomena (e.g., the growth and collapse of cavitation bubbles) [1,76].

Soft materials further enhance the environmental adaptability and safety of underwater robots [24,32]. Unlike traditional rigid carriers that are vulnerable in complex environments such as coral reefs and pipes, soft robots can deform to navigate through narrow gaps, and their flexible surfaces reduce damage to the environment and organisms [32,141]. Furthermore, soft materials typically possess high damping, absorbing water flow pulsations, thereby reducing vibrations and stabilizing the flow. Studies have shown that in turbulent water, the attitude fluctuations of flexible fish-shaped robots are significantly lower than those of equivalent rigid submersibles because their body oscillations can adapt to the impact of the water flow and absorb disturbance energy [1,145]. This adaptive capability is crucial for stabilizing sensor platforms and improving navigation accuracy in real-world sea conditions [32,145].

However, the application of soft materials also has limitations, particularly in terms of strength and lifespan: elastomers may degrade after prolonged immersion, and lower mechanical strength increases the risk of tearing [140,146,147]. Therefore, research has shifted towards composite materials, such as embedding fiber reinforcements in silicone or coating soft fins with wear-resistant layers, to balance flexibility and durability [32,147,148]. In summary, while new materials are injecting vitality into biomimetic propulsion, more experimental data are needed to quantify their effects. Many current research results are derived from ideal laboratory conditions, far removed from real-world marine applications [1,24,32]. For example, superhydrophobic coatings effective in clean water may fail in seawater due to fouling or bubble adhesion [93,140,142]. Biomimetic fish powered by smart materials in the laboratory are often small or require tethering, making long-term field operations impractical. Addressing these issues requires close collaboration and iterative development in materials science, fluid dynamics, and engineering design. Finally, as shown in Fig. 15, the integration of functional microstructure skin with a fully soft robotic architecture represents a key frontier for improving the hydrodynamic efficiency and environmental adaptability of underwater vehicles.

In conclusion, deformable/soft materials and bio-inspired surfaces offer novel avenues for enhancing the hydrodynamic performance of underwater bio-inspired robots. Through material innovation, we aim to engineer propulsion organs that closely mimic biology, endowing robots with bio-level efficiency and maneuverability. However, current evidence is primarily limited to principal verification and small-scale experiments, with a gap remaining before full-scale engineering application. The subsequent section will further discuss the limitations of existing research and outline future development directions [24,32,141].

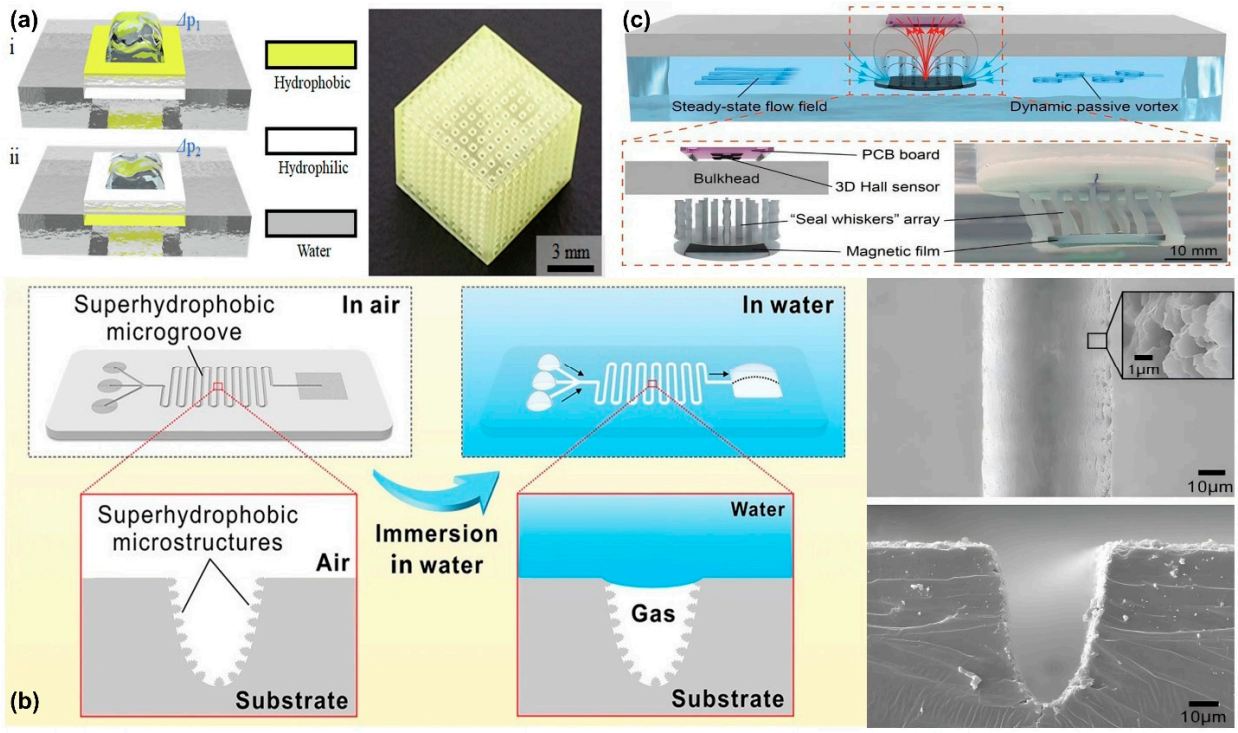

Figure 15: Functional skins and flow perception in biomimetic underwater robotics. (**a**) Hornwort-inspired unidirectional cellular fluidics for directional water transport. (**b**) Underwater aero-fluidic surface with superhydrophobic microgrooves for self-driven gas transport. (**c**) Seal-whisker-inspired hydrodynamic sensor for multidirectional flow and vortex-wake perception. Panels (**a**–**c**) are adapted with permission from Refs. [126,149,150], respectively.

6 Limitations of Current Evidence and Future Directions

Despite substantial progress in the hydrodynamics of bio-inspired underwater robots in recent years, a literature review reveals numerous common limitations that necessitate further investigation and resolution in future work [1].

Furthermore, beyond flapping propulsion, gliding and lift-based locomotion are utilized by certain species (e.g., rays) for long-distance, low-energy displacement. However, hydrodynamic evidence regarding these modes remains relatively fragmented within the bio-inspired robotics domain. Existing studies predominantly focus on idealized water tunnels or uniform flow conditions, lacking systematic comparisons of the coupling relationships among AoA, flexible wing deformation, and the lift-to-drag ratio (L/D) [15, 151,152].

First, the transferability of laboratory-scale evidence to real-ocean deployment remains insufficiently established. Many reviewed studies are conducted in quiescent water tanks, uniform-inflow water tunnels, or simplified numerical domains, where key variables such as Reynolds number, Strouhal number, inflow direction, turbulence intensity, and boundary conditions can be well controlled. These settings are essential for isolating fundamental mechanisms, including reverse Kármán vortex formation, leading-edge vortex attachment, flexibility-induced thrust enhancement, and biomimetic surface drag reduction. However, they do not fully represent realistic marine environments, where turbulence, oblique inflow, density stratification, and other factors coexist [145,153,154]. As a result, performance advantages demonstrated under idealized conditions may not be directly transferable to open-water operation. For example, incoming turbulence and wave-induced body motion may disturb vortex coherence and weaken thrust-vector alignment; oblique

inflow may change the effective angle of attack and generate asymmetric hydrodynamic loads; stratification may modify wake development and momentum transfer. Therefore, conclusions regarding high propulsive efficiency, stable wake organization, drag reduction, and maneuvering robustness should be interpreted as condition-dependent unless they are validated in turbulent flumes, wave basins, stratified-flow facilities, long-duration immersion tests, and field trials. Future studies should shift from mechanism verification under controlled laboratory conditions to the environmental robustness assessment of systems, and use comparable metrics under real ocean conditions to evaluate efficiency, maneuverability, material degradation, and other aspects.

Second, current numerical models and theoretical analyses predominantly focus on single propulsors or simplified operating conditions, resulting in an insufficient understanding of flow interference mechanisms in multi-propulsor, multi-degree-of-freedom systems [26,121,155]. In nature, fish often utilize body-caudal fin coordination or multi-fin synchronization, and wake interactions during schooling are highly complex. Conversely, existing robotics research often treats each propulsor in isolation, lacking comprehensive studies on multi-thruster interference effects [121]. For instance, how do interacting wake vortices alter thrust and efficiency when two flexible caudal fins swim at a specific separation distance? Can wake interference in robotic formations yield collective energy-saving effects? These questions remain largely unanswered. Although a few studies have preliminarily explored thrust augmentation in tandem wings and drag reduction in bio-inspired schooling, a generalized mechanism has yet to be established [121,155]. Future work requires increasing complexity in experiments and simulations to investigate unsteady flow fields under multi-flexible-propulsor arrangements, as well as vortex interference laws between propulsors and between robots. This has significant guiding significance for the design of swarm-intelligent underwater robots [26,121,155].

Third, regarding modeling and theoretical limitations, many current studies rely on idealized assumptions, restricting model applicability. For example, some CFD simulations employ two-dimensional approximations, ignoring three-dimensional effects; many theoretical analyses rely on potential flow or quasi-steady assumptions, failing to capture viscous vortex dissipation and turbulence generation [16]. These simplifications often lead to discrepancies between model predictions and experimental observations [115]. For instance, thrust predicted under potential flow assumptions is often higher than actual values due to the neglect of boundary layer friction and wake vortex energy dissipation. Furthermore, small-amplitude theories cannot explain LEV shedding and dynamic stall during large-amplitude flexible flapping. Among the 160 reviewed papers, many noted these limitations; for instance, Zhang et al. (2024) mentioned that CFD simulations struggle to fully reproduce experimentally measured fin-tip vortex structures, requiring higher resolution and improved turbulence models [1]. Future directions should involve developing more comprehensive theoretical frameworks that integrate viscous vortex dynamics, elastic structural waves, and active control. In addition, complex-fluid and non-Newtonian effects should be considered when bio-inspired robots operate in sediment-laden water, mucus-mediated boundary layers, polymer-assisted drag-reduction environments, or other particle-laden marine conditions. Recent numerical studies on bio-convective hybrid nanofluid flow provide a useful cross-disciplinary perspective for extending hydrodynamic models beyond ideal Newtonian-water assumptions [156]. Alternatively, data assimilation could be used to correct empirical terms in models using experimental data [115]. Beyond propulsion, theories regarding noise and vibration also require refinement. Current research on the acoustic characteristics of bio-inspired propulsion is scarce, yet stealth is crucial for practical applications. Future work should build acoustic prediction models to investigate the relationship between unsteady vortices and noise radiation.

Fourth, at the material and engineering implementation level, existing work remains largely at the prototype stage, lacking long-term, large-scale validation. Many bio-inspired robotic fish driven by smart materials can only demonstrate operation for minutes in a lab and have not solved issues regarding continuous, reliable operation. The power density and energy efficiency of electro-active materials lag behind electric motors; for example, IPMC-driven fish are slow, and SMA actuation cycles are long. The durability of flexible materials is another major challenge: long-term immersion causes elastomer aging and property changes, while marine bio-fouling can significantly reduce the efficacy of bio-inspired surfaces [32,157]. Therefore, future engineering efforts must develop superior material systems (e.g., highly water-fatigue-resistant elastomers, low-loss high-strength flexible composites) and subject prototypes to rigorous lifespan and environmental testing. Bio-inspired concepts can only achieve large-scale engineering application when propulsors demonstrate reliable performance advantages in real sea conditions over long cycles. Additionally, system integration warrants attention: the fusion of flexible bio-inspired propulsion with overall robot design (hull layout, control systems, energy systems) requires optimization. For instance, flexible fins need compatible attitude control algorithms, otherwise high maneuverability might lead to control difficulties [34,158]. Future exploration could involve Central Pattern Generator (CPG) control methods co-designed with bio-inspired propulsion hardware to achieve natural, fluid motion similar to fish [107].

In this context, AI-assisted optimization, machine learning, and digital-twin methods provide promising tools for addressing the high-dimensional design and control challenges of underwater bio-inspired robots. Recent studies on fish-like robots have shown that deep reinforcement learning and sim-to-real learning frameworks can be used to train path-following, pose-control, and flow-adaptive swimming policies, reducing the dependence on fully explicit hydrodynamic models. For flexible flapping propulsion, learning-based methods can also construct surrogate models or optimize actuation parameters, such as flapping frequency, amplitude, phase difference, stiffness distribution, and control policy, with lower computational cost than repeated high-fidelity CFD-FSI simulations. Digital twins further offer a route to integrate physical robots, hydrodynamic models, sensor feedback, and environmental data into a continuously updated virtual representation. Although digital-twin applications are currently more mature for conventional AUVs and ROVs than for fully bio-inspired robots, the same concept could be extended to fish-like and soft underwater robots for online performance prediction, energy-consumption estimation, fault diagnosis, material-fatigue monitoring, and adaptive control under changing flow conditions. However, practical implementation remains challenging because underwater bio-inspired robots involve strong FSI, limited onboard sensing, uncertain hydrodynamic loads, biofouling, material aging, and high computational demands for real-time model updating [159,160].

In summary, several key research directions in this field deserve close attention in the future:

1. Environmental robustness of biomimetic propulsion mechanisms: systematically evaluating vortex dynamics, thrust generation, efficiency, maneuverability, and control stability under turbulence, waves, oblique inflow, stratified flows, suspended particles, biofouling, and long-duration cyclic loading.
2. Flow coordination among multiple propellers and robots: including fluid dynamics energy-saving mechanisms in fish swarming and their biomimetic applications.
3. AI-assisted and digital-twin-enabled model fusion: developing comprehensive frameworks that combine CFD, nonlinear dynamics, machine learning, reinforcement learning, sensor feedback, and digital twins to enhance hydrodynamic prediction, control optimization, and online model updating.
4. Advanced materials and long-term operation: Developing high-performance flexible materials and actuators while addressing reliability and maintenance in marine environments.

5. Verification of bio-inspired mechanisms: Designing novel experiments to directly verify unclear mechanisms, such as the role of fin flexibility in turbulence or the skin compliance hypothesis, thereby guiding new theoretical construction.

7 Conclusion

Hydrodynamic research into underwater bio-inspired robots is progressively unveiling the secrets governing high-efficiency biological swimming, translating these mechanisms into innovative engineering solutions. In summary, through a systematic review of 160 relevant publications, this paper distills the following core conclusions:

1. Bio-inspired propulsion represents, in essence, the exploitation of unsteady flow dynamics. Organisms such as fish generate ordered vortex structures (e.g., Reverse Kármán vortex streets and vortex ring chains) via caudal undulation and fin oscillation, efficiently converting input energy into forward-directed momentum jets. This paradigm is fundamentally distinct from the operational mode of conventional propellers, which assumes steady flow conditions. Unsteady propulsion harnesses added mass effects and vortex dynamics to achieve superior thrust and efficiency; for instance, within an optimal Strouhal number range, the propulsive efficiency of oscillating fins significantly surpasses that of steady propellers. The analysis presented herein indicates that controlling the morphology of the wake vortex street is critical for enhancing performance—stable, ordered vortex trains signify directional energy output, whereas disordered, chaotic vortex fields indicate energy dissipation. Consequently, the design and control of bio-inspired robots should prioritize the generation and leverage of ideal vortex modes, thereby establishing new design criteria.
2. Flexible FSI constitutes the quintessence of underwater bio-inspired propulsion. The presence of flexible fins and compliant tails transforms the system from a mere forced oscillator into a complex coupled entity possessing adaptive capabilities and energy recovery mechanisms. Through passive deformation, flexible structures achieve compliance and modulation in response to fluid loads: they mitigate parasitic drag during propulsion (e.g., reducing negative thrust during stroke reversal) and recover kinetic energy via the storage and release of strain energy. Multiple studies cited in this review consistently demonstrate that appropriate flexibility significantly enhances propulsive efficiency and endows the robot with smoother thrust output. However, flexibility is not monotonically beneficial; rather, an optimal range exists. Future designers must leverage the advantages of flexibility while mitigating the performance degradation associated with excessive compliance. A pragmatic recommendation is to incorporate concepts of tunable or distributed flexibility, enabling the propulsor to maintain near-optimal compliance across varying operating conditions.
3. Novel materials and biomimetic surfaces have brought revolutionary opportunities to underwater robotics technology. Advances in materials science have spurred a wide variety of intelligent actuation materials and biomimetic coatings, endowing robots with biomimetic functional characteristics. Shape memory alloys (SMA) and dielectric elastomers (DE) enable muscle-like actuation, while flexible biomimetic skin and superhydrophobic coatings provide drag reduction effects similar to fish skin. The convergence of these technologies has propelled the “fully soft” biomimetic fish from concept to reality. Once the efficiency and reliability of material-based actuation are further improved, biomimetic robots will break through the limitations of traditional rigid machinery, moving freely in aquatic environments with forms highly similar to natural organisms.

While critically analyzing existing research, this review also outlines future developmental directions. It is foreseeable that the field of underwater bio-inspired robotics will increasingly exhibit a trend toward

interdisciplinary convergence, with a balanced emphasis on both engineering applications and fundamental research. For robotics researchers, a profound understanding of hydrodynamic mechanisms will serve as a continuous source of inspiration for novel designs; conversely, for fluid scientists, bio-inspired robots provide an ideal platform for validating theories and discovering new phenomena. This mutual reinforcement is destined to drive breakthrough advancements in the field. We anticipate that with the further elucidation of unsteady flow mysteries and the continuous optimization of flexible materials, future bio-inspired underwater robots will approach or even surpass natural organisms in efficiency, maneuverability, and stealth, thereby revolutionizing marine exploration and engineering applications. Researchers should uphold the fundamental biomimetic tenet of "learning from nature," continuing to explore and innovate at the nexus of fluid mechanics and bio-inspired engineering, ultimately realizing the design goal of robots that "swim as efficiently as fish."

Acknowledgement: The authors sincerely thank the researchers whose valuable work has been cited in this review, as well as the editor and the anonymous reviewers for their insightful comments and constructive suggestions.

Funding Statement: This work was funded by National Natural Science Foundation of China (Grant No. 52505320), Basic Research Program of Jiangsu (Grant No. BK20250734), Guangdong Basic and Applied Basic Research Foundation (Grant No. 2026A1515010218), China Postdoctoral Science Foundation (Grant No. 2025M780259), and Research Topics for 2025 of The Jiangsu Institution of Engineers (Grant No. JSIE2025KT10).

Author Contributions: Conceptualization, Hao Jiang, Liguo Shuai and Zhihan Li; methodology, Hao Jiang and Zhihan Li; software, Hao Jiang and Lucheng Sun; validation, Hao Jiang and Lucheng Sun; formal analysis, Hao Jiang; investigation, Hao Jiang and Lucheng Sun; resources, Liguo Shuai and Zhihan Li; data curation, Hao Jiang and Lucheng Sun; writing—original draft, Hao Jiang; writing—review and editing, Liguo Shuai and Zhihan Li; visualization, Hao Jiang and Lucheng Sun; supervision, Liguo Shuai and Zhihan Li; project administration, Liguo Shuai and Zhihan Li. All authors reviewed and approved the final version of the manuscript.

Availability of Data and Materials: No new data were created or analyzed in this study. Data sharing is not applicable.

Ethics Approval: Not applicable.

Conflicts of Interest: The authors declare no conflicts of interest to report regarding the present study.

References

1. Zhang Z, Wang Q, Zhang S. Review of computational fluid dynamics analysis in biomimetic applications for underwater vehicles. Biomimetics. 2024;9(2):79. [CrossRef].
2. Wang R, Wang S, Wang Y, Cheng L, Tan M. Development and motion control of biomimetic underwater robots: a survey. IEEE Trans Syst Man Cybern Syst. 2022;52(2):833–44. [CrossRef].
3. Ding H, Gao Q, Zhu Y, Shi H, Chen K, Chen R. Experimental study on navigation performance of bionic underwater vehicle inspired by sea turtle. Ocean Eng. 2024;310:118700. [CrossRef].
4. Anuat GV, Klamo JT, Pollman AG. Effects of body geometry and propulsion type on unmanned underwater vehicle interactions with marine vegetation. J Auton Veh Syst. 2022;2(2):021002. [CrossRef].
5. Li Z, Yan Y, Zhao Z, Xu Y, Hu Y. Numerical study on hydrodynamic effects of intermittent or sinusoidal coordination of pectoral fins to achieve spontaneous nose-up pitching behavior in dolphins. Ocean Eng. 2025;337:121854. [CrossRef].
6. Li Z, Xia D, Yang G, Wang X, Shi Y. Hydrodynamics of the self-diving function of thunniform swimmer relying on switching the caudal fin shape. J Mar Sci Technol. 2023;28(1):326–40. [CrossRef].
7. Yan H, Zhou Z, Lei M, Li Z, Xia D. Hydrodynamic Performance of cycloidal propellers with four-bar and mixed four-bar/five-bar mechanisms: a numerical study. J Appl Fluid Mech. 2024;17(3):628–45. [CrossRef].

8. Li G, Liu G, Leng D, Fang X, Li G, Wang W. Underwater undulating propulsion biomimetic robots: a review. Biomimetics. 2023;8(3):318. [CrossRef].
9. Triantafyllou MS, Triantafyllou GS. An efficient swimming machine. Sci Am. 1995;272(3):64–70. [CrossRef].
10. Fish FE. Advantages of natural propulsive systems. Mar Technol Soc J. 2013;47(5):37–44. [CrossRef].
11. Svendsen MBS, Domenici P, Marras S, Krause J, Boswell KM, Rodriguez-Pinto I, et al. Maximum swimming speeds of sailfish and three other large marine predatory fish species based on muscle contraction time and stride length: a myth revisited. Biol Open. 2016;5(10):1415–9. [CrossRef].
12. Sagong W, Jeon WP, Choi H. Hydrodynamic characteristics of the sailfish (*Istiophorus platypterus*) and swordfish (*Xiphias gladius*) in gliding postures at their cruise speeds. PLoS One. 2013;8(12):e81323. [CrossRef].
13. Lou J, Yang Y, Wu C, Li G, Chen T, Ma J. Underwater oscillation performance and 3D *Vortex* distribution generated by miniature caudal fin-like propulsion with macro fiber composite actuation. Sens Actuat A Phys. 2020;303:111587. [CrossRef].
14. Bai X, Wang Y, Wang R, Wang S, Tan M. Hydrodynamics of a flexible flipper for an underwater vehicle-manipulator system. IEEE/ASME Trans Mechatron. 2022;27(2):868–79. [CrossRef].
15. Xu T, Luo Y, Hou Z, Huang Q, Cao Y, Pan G. Research on passive deformation and hydrodynamic performance of a biomimetic cownose ray in gliding motion through fluid-structure interaction analysis. Phys Fluids. 2023;35(12):121905. [CrossRef].
16. Zeng Y, Hu Q, Zhang T, Li S, Shi X, Sun L, et al. Dynamic modeling and performance analysis of the undulating fin considering flexible deformation and fluid-fin interactions. Ocean Eng. 2025;320:120281. [CrossRef].
17. Qin Y, Tian Q, Shan M, Hu H. Numerical modeling of fluid-structure interactions by using a hybrid method of IB-LBM and ANCF. J Fluids Struct. 2025;137:104378. [CrossRef].
18. Kou J, Gu Y, Ren Y, Wu D, Wu Z, Mou J. Progress and future challenges in bionic drag reduction research inspired by fish skin properties. ACS Appl Mater Interfaces. 2025;17(38):54012–30. [CrossRef].
19. Chen Y, Hu Y, Zhang LW. Effective underwater drag reduction: a butterfly wing scale-inspired superhydrophobic surface. ACS Appl Mater Interfaces. 2024;16(20):26954–64. [CrossRef].
20. Xue Y, Li L, Zhang D, Liao WH, Guo X, Guo Y. Modeling and analysis of underwater oscillation of a flexible biomimetic caudal fin driven by MFC based on ANCF. Thin Walled Struct. 2026;218:113970. [CrossRef].
21. Breder CM. The locomotion of fishes. Zool Sci Contrib N Y Zool Soc. 1926;4(5):159–297. [CrossRef].
22. Webb PW. Form and function in fish swimming. Sci Am. 1984;251(1):72–82. [CrossRef].
23. Lamas MI, Rodriguez CG. Hydrodynamics of biomimetic marine propulsion and trends in computational simulations. J Mar Sci Eng. 2020;8(7):479. [CrossRef].
24. Ma S, Zhao Q, Ding M, Zhang M, Zhao L, Huang C, et al. A review of robotic fish based on smart materials. Biomimetics. 2023;8(2):227. [CrossRef].
25. Zhang T, Wang R, Wang Y, Cheng L, Wang S, Tan M. Design and locomotion control of a Dactylopteridae-inspired biomimetic underwater vehicle with hybrid propulsion. IEEE Trans Automat Sci Eng. 2022;19(3):2054–66. [CrossRef].
26. Li L, Li G, Li R, Xiao Q, Liu H. Multi-fin kinematics and hydrodynamics in pufferfish steady swimming. Ocean Eng. 2018;158:111–22. [CrossRef].
27. Chen YJ, Huang H, Bu W, Zhang X, Sheng C, Chen ZS. Kinematic modelling and hydrodynamic analysis of biomimetic pectoral fins of cownose ray. Ocean Eng. 2024;302:117577. [CrossRef].
28. Feng Y, Su Y. Numerical study on the turn maneuvering of a biomimetic robotic fish driven by pectoral fins in labriform mode under self-propulsion. Phys Fluids. 2025;37:011914. [CrossRef].
29. Scaradozzi D, Palmieri G, Costa D, Pinelli A. BCF swimming locomotion for autonomous underwater robots: a review and a novel solution to improve control and efficiency. Ocean Eng. 2017;130:437–53. [CrossRef].
30. Wang R, Wang S, Wang Y, Cai M, Tan M. Vision-based autonomous hovering for the biomimetic underwater robot—RobCutt-II. IEEE Trans Ind Electron. 2019;66(11):8578–88. [CrossRef].
31. Zhou C, Low KH. Design and locomotion control of a biomimetic underwater vehicle with fin propulsion. IEEE/ASME Trans Mechatron. 2012;17(1):25–35. [CrossRef].
32. Hasib SA, Gulzar MM, Oishy SR, Maaruf M, Habib S, Shakoor A. An investigation of innovative strategies in underwater soft robotics. Eng Sci Technol Int J. 2025;70:102123. [CrossRef].

33. Marchese AD, Onal CD, Rus D. Autonomous soft robotic fish capable of escape maneuvers using fluidic elastomer actuators. Soft Robot. 2014;1(1):75–87. [CrossRef].
34. Zhang T, Tian R, Yang H, Wang C, Sun J, Zhang S, et al. From simulation to reality: a learning framework for fish-like robots to perform control tasks. IEEE Trans Robot. 2022;38(6):3861–78. [CrossRef].
35. White CH, Lauder GV, Bart-Smith H. Tunabot Flex: a tuna-inspired robot with body flexibility improves high-performance swimming. Bioinspir Biomim. 2021;16(2):026019. [CrossRef].
36. Wang W, Xie G. Online high-precision probabilistic localization of robotic fish using visual and inertial cues. IEEE Trans Ind Electron. 2015;62(2):1113–24. [CrossRef].
37. Li Z, Xia D, Zhou Z. The Role of double-tentacled cooperative kinematics on the hydrodynamics of a self-propelled swimmer. J Appl Fluid Mech. 2023;16(6):1193–207. [CrossRef].
38. Li Z, Xia D, Kang S, Li Y, Li T. A comparative study of multi-tentacled underwater robot with different self-steering behaviors: maneuvering and cruising modes. Phys Fluids. 2024;36(11):115118. [CrossRef].
39. Gemmell BJ, Dabiri JO, Colin SP, Costello JH, Townsend JP, Sutherland KR. Cool your jets: biological jet propulsion in marine invertebrates. J Exp Biol. 2021;224(12):jeb222083. [CrossRef].
40. Serchi FG, Arienti A, Laschi C. Biomimetic *Vortex* propulsion: toward the new paradigm of soft unmanned underwater vehicles. IEEE/ASME Trans Mechatron. 2013;18(2):484–93. [CrossRef].
41. Dabiri JO, Colin SP, Costello JH, Gharib M. Flow patterns generated by oblate medusan jellyfish: field measurements and laboratory analyses. J Exp Biol. 2005;208(7):1257–65. [CrossRef].
42. Dabiri JO. On the estimation of swimming and flying forces from wake measurements. J Exp Biol. 2005;208(18):3519–32. [CrossRef].
43. Luo K, Yan L, Zhu Z, Hua X, Wang Z, Wang H, et al. Design and optimization of a bionic jellyfish robot for enhanced underwater propulsion efficiency. Ocean Eng. 2025;340:122414. [CrossRef].
44. Yuk H, Lin S, Ma C, Takaffoli M, Fang NX, Zhao X. Hydraulic hydrogel actuators and robots optically and sonically camouflaged in water. Nat Commun. 2017;8:14230. [CrossRef].
45. Ye J, Yao YC, Gao JY, Chen S, Zhang P, Sheng L, et al. LM-jelly: liquid metal enabled biomimetic robotic jellyfish. Soft Robot. 2022;9(6):1098–107. [CrossRef].
46. Shen Z, Na J, Wang Z. A biomimetic underwater soft robot inspired by cephalopod mollusc. IEEE Robot Autom Lett. 2017;2(4):2217–23. [CrossRef].
47. Wang T, Joo HJ, Song S, Hu W, Keplinger C, Sitti M. A versatile jellyfish-like robotic platform for effective underwater propulsion and manipulation. Sci Adv. 2023;9(15):eadg0292. [CrossRef].
48. Read DA, Hover FS, Triantafyllou MS. Forces on oscillating foils for propulsion and maneuvering. J Fluids Struct. 2003;17(1):163–83. [CrossRef].
49. Lai YH, Lan B, Chiang CY, Hsu DY. Enhancing underwater unmanned vehicle efficiency through asymmetric dynamics in *Manta*-like swimming. Phys Fluids. 2024;36(10):101902. [CrossRef].
50. Taylor GK, Nudds RL, Thomas ALR. Flying and swimming animals cruise at a Strouhal number tuned for high power efficiency. Nature. 2003;425(6959):707–11. [CrossRef].
51. Schouveiler L, Hover FS, Triantafyllou MS. Performance of flapping foil propulsion. J Fluids Struct. 2005;20(7):949–59. [CrossRef].
52. Triantafyllou GS, Triantafyllou MS, Grosenbaugh MA. Optimal thrust development in oscillating foils with application to fish propulsion. J Fluids Struct. 1993;7(2):205–24. [CrossRef].
53. Bhamra NS, Vijayan K. Underwater bio-inspired propulsion using actuation of coupled structures. Ocean Eng. 2025;331:121351. [CrossRef].
54. Krishnadas A, Ravichandran S, Rajagopal P. Analysis of biomimetic caudal fin shapes for optimal propulsive efficiency. Ocean Eng. 2018;153:132–42. [CrossRef].
55. Chen L, Hu Q, Li S, Zhang H, Sun L, Wei H, et al. Underwater bionic undulating fins incorporating thickness effects: hydrodynamic performance and optimal thickness variation rate analysis. Bioinspir Biomim. 2025;20(4):046006. [CrossRef].
56. Jaya AS, Kartidjo MW. Thrust and efficiency enhancement scheme of the fin propulsion of the biomimetic Autonomous Underwater Vehicle model in low-speed flow regime. Ocean Eng. 2022;243:110090. [CrossRef].

57. Karbasian HR, Kim KC. Numerical investigations on flow structure and behavior of vortices in the dynamic stall of an oscillating pitching hydrofoil. Ocean Eng. 2016;127:200–11. [CrossRef].
58. Ducoin A, Young YL. Hydroelastic response and stability of a hydrofoil in viscous flow. J Fluids Struct. 2013;38:40–57. [CrossRef].
59. Geissler W, van der Wall BG. Dynamic stall control on flapping wing airfoils. Aerosp Sci Technol. 2017;62:1–10. [CrossRef].
60. Young JD, Morris SE, Schutt RR, Williamson CHK. Effect of hybrid-heave motions on the propulsive performance of an oscillating airfoil. J Fluids Struct. 2019;89:203–18. [CrossRef].
61. Zhang M, Liu T, Huang B, Wu Q, Wang G. Hydrodynamic characteristics and flow structures of pitching hydrofoil with special emphasis on the added force effect. Renew Energy. 2020;157:560–73. [CrossRef].
62. Zhang T, Hu Q, Li S, Zhao J, Zeng Y, Zu S, et al. Influence of hydrofoil motion patterns on the hydrodynamic performance of undulating fin for biomimetic underwater robots. Ocean Eng. 2024;314:119694. [CrossRef].
63. Rayapureddi R, Mitra S. Evolution of maneuverability for biomimetic underwater soft robots. Phys Fluids. 2025;37(9):097175. [CrossRef].
64. Dong H, Wu Z, Tan M, Yu J. Hydrodynamic analysis and verification of an innovative whale shark-like underwater glider. J Bionic Eng. 2020;17(1):123–33. [CrossRef].
65. Yang S, Wang X, Miao Z, Chen Y, Sun T, Wang P, et al. Drag reduction mechanism of the biomimetic superhydrophobic surface on the boundary layer of underwater gliders. Phys Fluids. 2025;37(2):025154. [CrossRef].
66. Zhang Y, Su C, Zou Z, Li J, Ji M, Song X, et al. Underwater biomimetic structures and surface technologies: a frontier review from natural inspiration to engineering implementation. Ocean Eng. 2025;334:121591. [CrossRef].
67. Choi H, Park H, Sagong W, Lee SI. Biomimetic flow control based on morphological features of living creatures. Phys Fluids. 2012;24(12):121302. [CrossRef].
68. Oeffner J, Lauder GV. The hydrodynamic function of shark skin and two biomimetic applications. J Exp Biol. 2012;215(5):785–95. [CrossRef].
69. Dean B, Bhushan B. Shark-skin surfaces for fluid-drag reduction in turbulent flow: a review. Phil Trans R Soc A. 2010;368(1929):4775–806. [CrossRef].
70. Pavlov VV. Dolphin skin as a natural anisotropic compliant wall. Bioinspir Biomim. 2006;1(2):31–40. [CrossRef].
71. Wang D, Liu H. Dolphin-inspired skin microvibrations offer a novel pressure-dominated drag reduction mechanism. J Bionic Eng. 2025;22(2):793–804. [CrossRef].
72. Zhang D, Xie Y, Zhang Y, Liang Z, Tian Y. Experimental advances in airfoil dynamic stall and transition phenomena. Fluid Dyn Mater Process. 2025;21(4):697–739. [CrossRef].
73. Gardner AD, Jones AR, Mulleners K, Naughton JW, Smith MJ. Review of rotating wing dynamic stall: experiments and flow control. Prog Aerosp Sci. 2023;137:100887. [CrossRef].
74. Alberti L, Carnevali E, Costa D, Crivellini A. A computational fluid dynamics investigation of a flapping hydrofoil as a thruster. Biomimetics. 2023;8(2):135. [CrossRef].
75. Wang H, Zheng X, Pröbsting S, Hu C, Wang Q, Li Y. An unsteady RANS simulation of the performance of an oscillating hydrofoil at a high Reynolds number. Ocean Eng. 2023;274:114097. [CrossRef].
76. Zhu D, Zhao L, Feng X, Tian G. Experimental study of turbulent drag reduction characteristics of biomimetic divergent spines surfaces based on particle image velocimetry and proper orthogonal decomposition. Ocean Eng. 2024;311:119007. [CrossRef].
77. Shinde SY, Arakeri JH. Flexibility in flapping foil suppresses meandering of induced jet in absence of free stream. J Fluid Mech. 2014;757:231–50. [CrossRef].
78. Li Y, Song J, Yin L, Jin B, Yin B, Zhong Y. Hydrodynamics and musculature actuation of fish during a fast start. Appl Sci. 2023;13(4):2365. [CrossRef].
79. Feng YK, Liu HX, Su YY, Su YM. Numerical study on the hydrodynamics of C-turn maneuvering of a tuna-like fish body under self-propulsion. J Fluids Struct. 2020;94:102954. [CrossRef].
80. Walker JA. Does a rigid body limit maneuverability? J Exp Biol. 2000;203(22):3391–6. [CrossRef].
81. Li ZG, Ma WJ, Ge LM, Du YJ. Research on turning characteristics of a biomimetic robotic boxfish driven by pectoral fin with two degrees of freedom. Robot. 2016;38(5):593–602. (In Chinese). [CrossRef].

82. Hao Y, Cao Y, Cao Y, Huang Q, Pan G. Course control of a *Manta* Robot based on amplitude and phase differences. J Mar Sci Eng. 2022;10(2):285. [CrossRef].
83. Lua KB, Lu H, Zhang XH, Lim TT, Yeo KS. Aerodynamics of two-dimensional flapping wings in tandem configuration. Phys Fluids. 2016;28(12):121901. [CrossRef].
84. Babu Mannam NP, Alam MM, Krishnankutty P. Review of biomimetic flexible flapping foil propulsion systems on different planetary bodies. Results Eng. 2020;8:100183. [CrossRef].
85. Zhang Y, Lauder GV. Energy conservation by collective movement in schooling fish. eLife. 2024;12:RP90352. [CrossRef].
86. Zhang Y, Ko H, Calicchia MA, Ni R, Lauder GV. Collective movement of schooling fish reduces the costs of locomotion in turbulent conditions. PLoS Biol. 2024;22(6):e3002501. [CrossRef].
87. Lin X, Liao H, Xie H, Wu J. The impact of wavelength and phase difference on the collective performance of two parallel fish. J Fluid Mech. 2026;1032:A47. [CrossRef].
88. Fish FE, Lauder GV. Control surfaces of aquatic vertebrates: active and passive design and function. J Exp Biol. 2017;220(23):4351–63. [CrossRef].
89. Wainwright DK, Lauder GV, Gemmell BJ. Hydrodynamic function of the slimy and scaly surfaces of teleost fishes. Integr Comp Biol. 2024;64(2):480–95. [CrossRef].
90. Zhang Y, Feng X, Tian G, Jia C. Rheological properties and drag reduction performance of puffer epidermal mucus. ACS Biomater Sci Eng. 2022;8(2):460–9. [CrossRef].
91. Zhang L, Wan X, Zhou X, Cao Y, Duan H, Yan J, et al. Pyramid-shaped superhydrophobic surfaces for underwater drag reduction. ACS Appl Mater Interfaces. 2024;16(33):44319–27. [CrossRef].
92. Tian G, Shi J, Hu Y, Zhou H, Feng X. Numerical-experimental study on the influence of the Biomimetic spine-covered Protrusions (BSCPs) structure on the base pressure and near-wake flow of Underwater vehicles. Arab J Sci Eng. 2022;47(6):6821–35. [CrossRef].
93. Shi H, Zhang H, Geng L, Qu S, Wang X, Nikrityuk PA. Dynamic behaviors of cavitation bubbles near biomimetic surfaces: a numerical study. Ocean Eng. 2024;292:116628. [CrossRef].
94. Vilumbrales-Garcia R, Sudarsana PB, Sareen A. Adaptive drag reduction of a sphere using smart morphable skin. Flow. 2025;5:E17. [CrossRef].
95. Lighthill MJ. Note on the swimming of slender fish. J Fluid Mech. 1960;9(2):305–17. [CrossRef].
96. Theodorsen T. General theory of aerodynamic instability and the mechanism of flutter. Washington, DC, USA: NASA Reference Publication; 1935. Report No.: NACA-TR-496.
97. Wu TYT. Hydromechanics of swimming propulsion. Part 1. Swimming of a two-dimensional flexible plate at variable forward speeds in an inviscid fluid. J Fluid Mech. 1971;46(2):337–55. [CrossRef].
98. Hu J, Xu Y, Chen P, Xie F, Li H, He K. Design and reality-based modeling optimization of a flexible passive joint paddle for swimming robots. Biomimetics. 2024;9(1):56. [CrossRef].
99. Zhong Y, Du R. Design and implementation of a novel robot fish with active and compliant propulsion mechanism. Robot Sci Syst. 2016;12:1–9. [CrossRef].
100. Qu Y, Xie X, Zhang S, Xing C, Cao Y, Cao Y, et al. A rigid-flexible coupling dynamic model for robotic *Manta* with flexible pectoral fins. J Mar Sci Eng. 2024;12(2):292. [CrossRef].
101. Meng H, Lou J, Chen T, Xu C, Chen H, Yang Y, et al. Cantilever-based micro thrust measurement and pressure field distribution of biomimetic robot fish actuated by macro fiber composites (MFCs) actuators. Smart Mater Struct. 2021;30(3):035001. [CrossRef].
102. Saeed A, Farooq H, Akhtar I, Tariq MA, Khalid MSU. Deep-learning-based reduced-order model for power generation capacity of flapping foils. Biomimetics. 2023;8(2):237. [CrossRef].
103. Lucas KN, Thornycroft PJM, Gemmell BJ, Colin SP, Costello JH, Lauder GV. Effects of non-uniform stiffness on the swimming performance of a passively-flexing, fish-like foil model. Bioinspir Biomim. 2015;10(5):056019. [CrossRef].
104. Park YJ, Jeong U, Lee J, Kwon SR, Kim HY, Cho KJ. Kinematic condition for maximizing the thrust of a robotic fish using a compliant caudal fin. IEEE Trans Robot. 2012;28(6):1216–27. [CrossRef].
105. Esposito CJ, Tangorra JL, Flammang BE, Lauder GV. A robotic fish caudal fin: effects of stiffness and motor program on locomotor performance. J Exp Biol. 2012;215(1):56–67. [CrossRef].

106. Park YJ, Huh TM, Park D, Cho KJ. Design of a variable-stiffness flapping mechanism for maximizing the thrust of a bio-inspired underwater robot. Bioinspir Biomim. 2014;9(3):036002. [CrossRef].
107. Lu P, Dong B, Gao X, Zhang F, Song Y, Liu Z, et al. Variable-stiffness underwater robotic systems: a review. J Mar Sci Eng. 2025;13(9):1805. [CrossRef].
108. Liu Y, Jiang H, Xu Z. Development of novel fish-inspired robot with variable stiffness. Ocean Eng. 2024;305:118047. [CrossRef].
109. Reddy NS, Sen S, Har C. Effect of flexural stiffness distribution of a fin on propulsion performance. Mech Mach Theory. 2018;129:218–31. [CrossRef].
110. Piskur P. Side fins performance in biomimetic unmanned underwater vehicle. Energies. 2022;15(16):5783. [CrossRef].
111. Lucas KN, Johnson N, Beaulieu WT, Cathcart E, Tirrell G, Colin SP, et al. Bending rules for animal propulsion. Nat Commun. 2014;5:3293. [CrossRef].
112. Zheng C, Ding J, Dong B, Lian G, He K, Xie F. How non-uniform stiffness affects the propulsion performance of a biomimetic robotic fish. Biomimetics. 2022;7(4):187. [CrossRef].
113. Cha Y, Chae W, Kim H, Walcott H, Peterson SD, Porfiri M. Energy harvesting from a piezoelectric biomimetic fish tail. Renew Energy. 2016;86:449–58. [CrossRef].
114. Simha A, Gkliva R, Kotta U, Kruusmaa M. A flapped paddle-fin for improving underwater propulsive efficiency of oscillatory actuation. IEEE Robot Autom Lett. 2020;5(2):3176–81. [CrossRef].
115. Zhou P, Ren H, Fan W, Zhang Z. Multi-field coupled dynamic modeling of hard-magnetic beams interacting with fluid and its application to a magnetic-driven biomimetic jellyfish robot. Appl Math Model. 2025;148:116266. [CrossRef].
116. Maertens AP, Triantafyllou MS, Yue DP. Efficiency of fish propulsion. Bioinspir Biomim. 2015;10(4):046013. [CrossRef].
117. Roberts TJ, Azizi E. Flexible mechanisms: the diverse roles of biological springs in vertebrate movement. J Exp Biol. 2011;214(3):353–61. [CrossRef].
118. Szymak P, Piskur P, Kot R, Naus K, Powarzyński D. Biomimetic propulsion system efficiency for unmanned underwater vehicle. Sci Rep. 2025;15:11086. [CrossRef].
119. Moreira D, Mathias N, Morais T. Dual flapping foil system for propulsion and harnessing wave energy: A 2D parametric study for unaligned foil configurations. Ocean Eng. 2020;215:107875. [CrossRef].
120. Blake RW. Fish functional design and swimming performance. J Fish Biol. 2004;65(5):1193–222. [CrossRef].
121. Maertens AP, Gao A, Triantafyllou MS. Optimal undulatory swimming for a single fish-like body and for a pair of interacting swimmers. J Fluid Mech. 2017;813:301–45. [CrossRef].
122. Li Y, Qiu L, He Y, Dai S. Mechanism motion scheme design and dynamic analysis of biomimetic jellyfish adapt to different application. Mech Mach Theory. 2024;194:105584. [CrossRef].
123. Gemmell BJ, Costello JH, Colin SP, Stewart CJ, Dabiri JO, Tafti D, et al. Passive energy recapture in jellyfish contributes to propulsive advantage over other metazoans. Proc Natl Acad Sci U S A. 2013;110(44):17904–9. [CrossRef].
124. Zhong Q, Zhu J, Fish FE, Kerr SJ, Downs AM, Bart-Smith H, et al. Tunable stiffness enables fast and efficient swimming in fish-like robots. Sci Robot. 2021;6(57):eabe4088. [CrossRef].
125. Li N, Zhuang J, Zhu Y, Su G, Su Y. Fluid dynamics of a self-propelled biomimetic underwater vehicle with pectoral fins. J Ocean Eng Sci. 2021;6(2):160–9. [CrossRef].
126. Xie M, Duan H, Cheng P, Chen Y, Dong Z, Wang Z. Underwater unidirectional cellular fluidics. ACS Appl Mater Interfaces. 2022;14(7):9891–8. [CrossRef].
127. Wang B, Li L, Xu M, Hu N, Gao W, Zhang J, et al. Adaptive multimodal swimming gaits in a reconfigurable modular soft robotic fish. Sci Adv. 2026;12:eaea1299. [CrossRef].
128. Zheng Z, Gu X, Yang S, Wang Y, Zhang Y, Han Q, et al. Underwater drag reduction applications and fabrication of bio-inspired surfaces: a review. Biomimetics. 2025;10(7):470. [CrossRef].
129. Liu X, Li J, Xing Y, Zhang Z, Cao Y, Cao Y, et al. Soft biomimetic underwater vehicles: a review of actuation mechanisms, structure designs and underwater applications. Micromachines. 2026;17(2):258. [CrossRef].

130. Bernat J, Gajewski P, Kołota J, Marcinkowska A. Review of soft actuators controlled with electrical stimuli: IPMC, DEAP, and MRE. Appl Sci. 2023;13(3):1651. [CrossRef].
131. Youn JH, Jeong SM, Hwang G, Kim H, Hyeon K, Park J, et al. Dielectric elastomer actuator for soft robotics applications and challenges. Appl Sci. 2020;10(2):640. [CrossRef].
132. Shen Q, Wang T, Kim KJ. A biomimetic underwater vehicle actuated by waves with ionic polymer–metal composite soft sensors. Bioinspir Biomim. 2015;10(5):055007. [CrossRef].
133. Wang R, Zhang C, Zhang Y, Tan W, Chen W, Liu L. Soft underwater swimming robots based on artificial muscle. Adv Mater Technol. 2023;8(4):2200962. [CrossRef].
134. Ye Z, Hou P, Chen Z, Member I. 2D maneuverable robotic fish propelled by multiple ionic polymer–metal composite artificial fins. Int J Intell Robot Appl. 2017;1(2):195–208. [CrossRef].
135. Coral W, Rossi C, Curet OM, Castro D. Design and assessment of a flexible fish robot actuated by shape memory alloys. Bioinspir Biomim. 2018;13(5):056009. [CrossRef].
136. Chen Z. A review on robotic fish enabled by ionic polymer–metal composite artificial muscles. Robot Biomim. 2017;4(1):24. [CrossRef].
137. Cha Y, Porfiri M. Mechanics and electrochemistry of ionic polymer metal composites. J Mech Phys Solids. 2014;71:156–78. [CrossRef].
138. Wang Z, Hang G, Li J, Wang Y, Xiao K. A micro-robot fish with embedded SMA wire actuated flexible biomimetic fin. Sens Actuat A Phys. 2008;144(2):354–60. [CrossRef].
139. Li X, Rao D, Zhang M, Xue Y, Cao X, Yin S, et al. A jelly-like artificial muscle for an untethered underwater robot. Cell Rep Phys Sci. 2024;5(5):101957. [CrossRef].
140. Haghighi AH, Mobaraki V, Shayegani SMR, Sharif M. Introducing the elastomers with lowest water absorption and permeability. Results Chem. 2025;16:102485. [CrossRef].
141. Katzschmann RK, DelPreto J, MacCurdy R, Rus D. Exploration of underwater life with an acoustically controlled soft robotic fish. Sci Robot. 2018;3(16):eaar3449. [CrossRef].
142. Qu J, He P, Sun R, Huang K, Zhao J, Mo J. A laser-induced superhydrophobic surface with multiple microstructures for stable drag reduction. Surf Coat Technol. 2024;490:131181. [CrossRef].
143. Asidin MA, Suali E, Jusnukin T, Lahin FA. Review on the applications and developments of drag reducing polymer in turbulent pipe flow. Chin J Chem Eng. 2019;27(8):1921–32. [CrossRef].
144. Meng J, Wang J, Lyu C, Zhou Z, Wang L, Nie B. Characteristics and influencing factors of interaction between hydrophobic surface and drag-reducing polymer: a MC and MD simulation study. Comput Mater Sci. 2023;230:112473. [CrossRef].
145. Zheng J, Zhang T, Wang C, Xiong M, Xie G. Learning for attitude holding of a robotic fish: an end-to-end approach with sim-to-real transfer. IEEE Trans Robot. 2022;38(2):1287–303. [CrossRef].
146. Wang C, Xu Z, Xia Y, Zhang C, Fang H, Sun K. Water transport mechanism and performance evaluation in polyurethane materials: a state-of-the-art review. Polym Test. 2024;138:108554. [CrossRef].
147. Kumar R, Rezapourian M, Rahmani R, Maurya HS, Kamboj N, Hussainova I. Bioinspired and multifunctional tribological materials for sliding, erosive, machining, and energy-absorbing conditions: a review. Biomimetics. 2024;9(4):209. [CrossRef].
148. Wani IN, Aggarwal K, Bishnoi S, Shukla PK, Harursampath D, Garg A. Materials used in space shuttle: evolution, challenges, and future prospects—an overview. Compos Part B Eng. 2025;303:112540. [CrossRef].
149. Yong J, Peng Y, Wang X, Li J, Hu Y, Chu J, et al. Self-driving underwater "aerofluidics". Adv Sci. 2023;10(21):2301175. [CrossRef].
150. Dai H, Zhang C, Hu H, Hu Z, Sun H, Liu K, et al. Biomimetic hydrodynamic sensor with whisker array architecture and multidirectional perception ability. Adv Sci. 2024;11(38):2405276. [CrossRef].
151. Cai WH, Zhan JM, Luo YY. A study on the hydrodynamic performance of *Manta* ray biomimetic glider under unconstrained six-DOF motion. PLoS One. 2020;15(11):e0241677. [CrossRef].
152. Rozhdestvensky K, Zhao B. Recent advances in hydrodynamics of wing propulsive lifting systems for ships and underwater vehicles. Phys Fluids. 2023;35(11):111302. [CrossRef].
153. Shi X, Chen Z, Zhang T, Li S, Zeng Y, Chen L, et al. Hydrodynamic performance of a biomimetic undulating fin robot under different water conditions. Ocean Eng. 2023;288:116068. [CrossRef].

154. Wei H, Guo C, Han Y, Wu Y, Zheng X, Wang C. Influence of the stratification parameters on the wake field of an underwater vehicle in a two-layer stratified flow. Ocean Eng. 2024;312:119000. [CrossRef].
155. Li L, Nagy M, Graving JM, Bak-Coleman J, Xie G, Couzin ID. *Vortex* phase matching as a strategy for schooling in robots and in fish. Nat Commun. 2020;11:5408. [CrossRef].
156. Singh A, Yadav PK. Analysis of bio-convective ternary hybrid nanofluid flow in atherosclerotic bifurcated artery: a numerical approach. Comput Meth Programs Biomed. 2026;273:109129. [CrossRef].
157. Yao Q, Xiao S, Zeng Z, Ji Z, Jiang S, Shan F. A review of particle image velocimetry in fish-inspired biomimetic propulsion. Ocean Eng. 2025;341:122463. [CrossRef].
158. Zhang T, Hu Q, Li S, Wei C, Zu S, Shi X. A CPG-based framework for flexible locomotion control and propulsion performance evaluation of underwater undulating fin platform. Ocean Eng. 2023;288:116118. [CrossRef].
159. Zhang T, Tian R, Wang C, Xie G. Path-following control of fish-like robots: a deep reinforcement learning approach. IFAC-PapersOnLine. 2020;53(2):8163–8. [CrossRef].
160. Cui X, Sun B, Zhu Y, Yang N, Zhang H, Cui W, et al. Enhancing efficiency and propulsion in bio-mimetic robotic fish through end-to-end deep reinforcement learning. Phys Fluids. 2024;36(3):031910. [CrossRef].